UNIVERSITY COLLEGE LONDON

DEPARTMENT OF MATHEMATICS

Unsteady finite amplitude wave packets in a nonlinear equation from rotating flows

Author:
Mr. Calvin CHUNIA
Supervisor:
Prof. E. R. JOHNSON

March 11, 2021

Contents

Chapter 1

Introduction

Researchers have observed internal waves from rotating flows for many years to analyse their generation and evolution. Nonlinear equations can model such flows, the solutions of which form wave packets that propagate within a frame of reference. The aim of this project is to solve an equation of this type with the aid of numerical integration.

1.1 Internal Waves

Internal waves behave like surface waves, but instead of propagating along the interface between water and air, they manifest themselves on internal surfaces of lakes and oceans at generally lower frequencies and larger amplitudes, where internal surfaces are layers of water in which the changes in density are rapid with increasing depth [12].

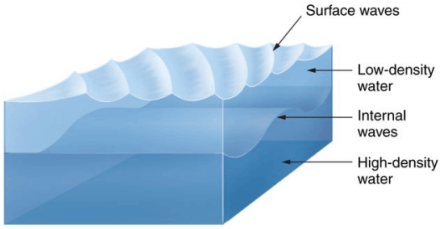

Figure 1.1: Visual interpretation of internal waves [1]

1.1.1 Internal Waves in the South China Sea

The reason why we are interested in internal waves lies in the observations made in the South China Sea. In the deep basin of this sea, a special type of internal wave called internal tides appears. Internal tides occur at tidal frequencies and are generally generated when tides at the surface move layers of water up and down [11]. The ones produced in Luzon Strait, which lies between Taiwan and the Philippines, generate internal tides which become steep under the effect of non-linearity, rotation, and non-hydrostatic dispersion as they travel west, forming one or more soliton pulses and evolve into high-frequency non-linear internal waves [9].

Luzon Strait contains two ridges: Lan-Yu Ridge to the east and Heng-Chun Ridge on the western side of the strait. The southern part of Lan-Yu ridge and the southern part of Heung-Chun Ridge contain shallow water and the strong tidal currents that occur in these shallow passes actively generate the observed internal waves [5].

Observations in Luzon Strait on internal waves continued for years, not only due to people not being able to discover the truth behind their generation or variability since the flow conditions were not ideal [4], which made measurements hard to take, but also because these waves have a direct impact on the environment: they affect the distributions of plankton in the oceans, can carry nutritions for aquatic plants to perform photosynthesis, directly affecting the population of plants underwater... and so on [2].

These internal waves form wave packets and not solitons: once the wave becomes too steep due to the non-linearity, the non-hydrostatic effect allows it to evolve into a non-linear wave train (wave-packets) [5].

Figure 1.2: Luzon Strait, South China Sea [3]

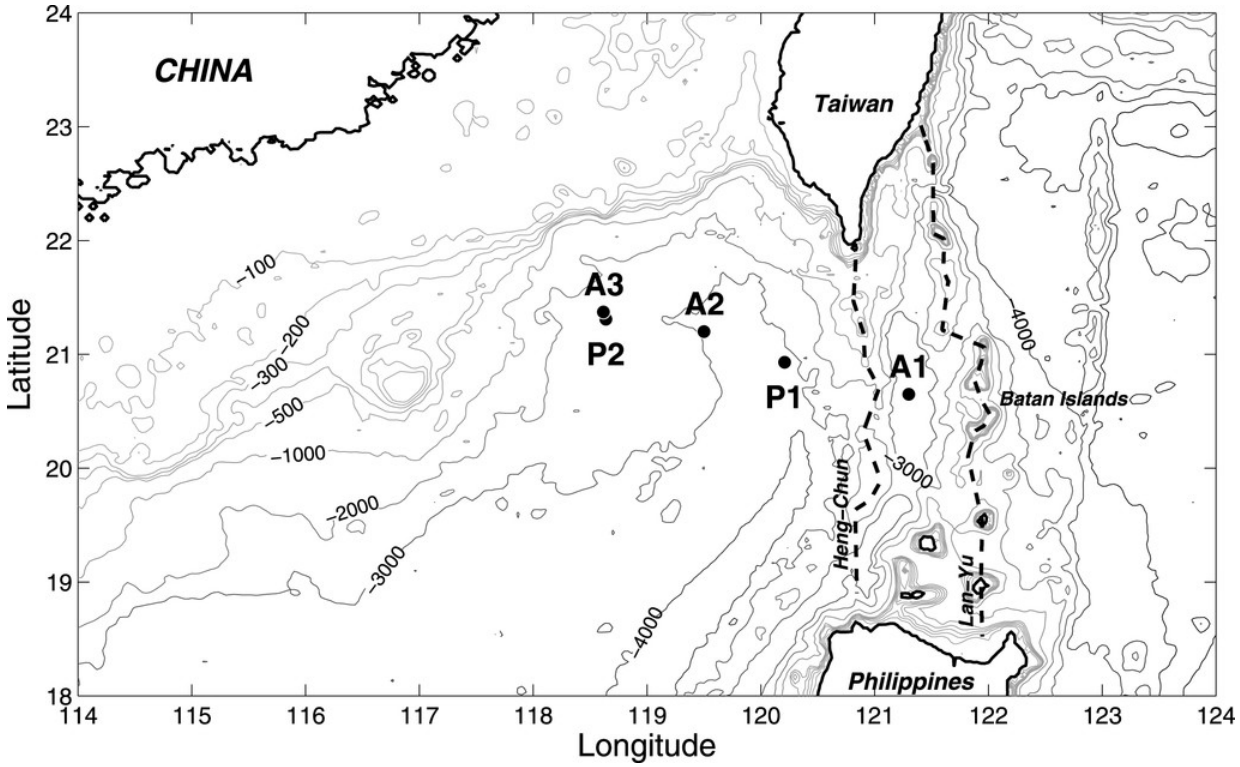

Figure 1.3: Ridges in Luzon Strait [9]

1.2 Linear Wave-packets

Let's consider a superposition of two linear waves of the form

$$\eta(x,t) = A\cos[(k-\delta)x - (\omega-\epsilon)t] + A\cos[(k+\delta)x - (\omega+\epsilon)t] \tag{1.2.1}$$

where $\delta \ll k$, $\epsilon \ll \omega$ and $A,\ \delta,\ k,\ \epsilon,\ \omega$ are all constants.
Applying the double angle formula given as

$$\cos(B \pm C) = \cos(B)\cos(C) \mp \sin(B)\sin(C) \tag{1.2.2}$$

equation (1.9) becomes

$$\eta(x,t) = 2A\cos(kx - \omega t)\cos(\delta x - \epsilon t) \tag{1.2.3}$$

The envelope of this wave-packet is given by $\pm|2A\cos(\delta x - \epsilon t)|$ and it moves with speed $c_g = \epsilon/\delta$. We call c_g the group velocity of the wave-packet and we can also calculate it by considering the ratio between the change in angular frequency and the change in angular wave-number:

$$c_g = \frac{\partial\omega}{\partial k} \tag{1.2.4}$$

The phase is instead given by the carrier wave, $\cos(kx - \omega t)$, with phase speed $c_p = \omega/k$.

Figure 1.4 shows an example of a linear wave packet. The wave is given by

$$\eta(x,t) = 2\cos(x - t)\cos(0.1x - 0.5t) \tag{1.2.5}$$

and we took snapshots of the function at $t = 0$ and $t = 1$. In both pictures, the red line represents the envelope, here given by $\pm|2A\cos(0.1x - 0.5t)|$, and the blue line the wave-packet. In Figure 1.4 (a), the black circle corresponds to a point that exists on the envelope but also on the wave at $t = 0$, while in (b), the red and blue circles show where that point has moved along the envelope and along the wave respectively at $t = 1$.

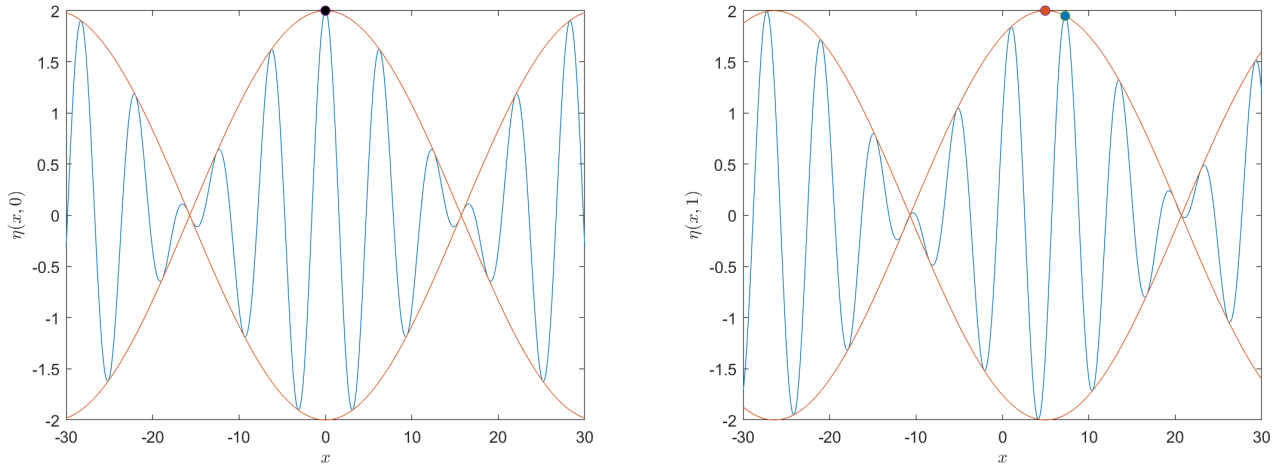

(a) (b)

Figure 1.4: Snapshots at $t = 0$ (a) and $t = 1$ (b) of (1.2.5)

For this example, the phase speed is $c_p = 1$ and the group velocity is $c_g = 5$, so the wave and the envelope move at different speeds as expected.

1.3 Non-linear Wave-packets

Non-linear wave-packets behave in the same way as linear ones, but the function representing the envelope of the wave is typically not sinusoidal.

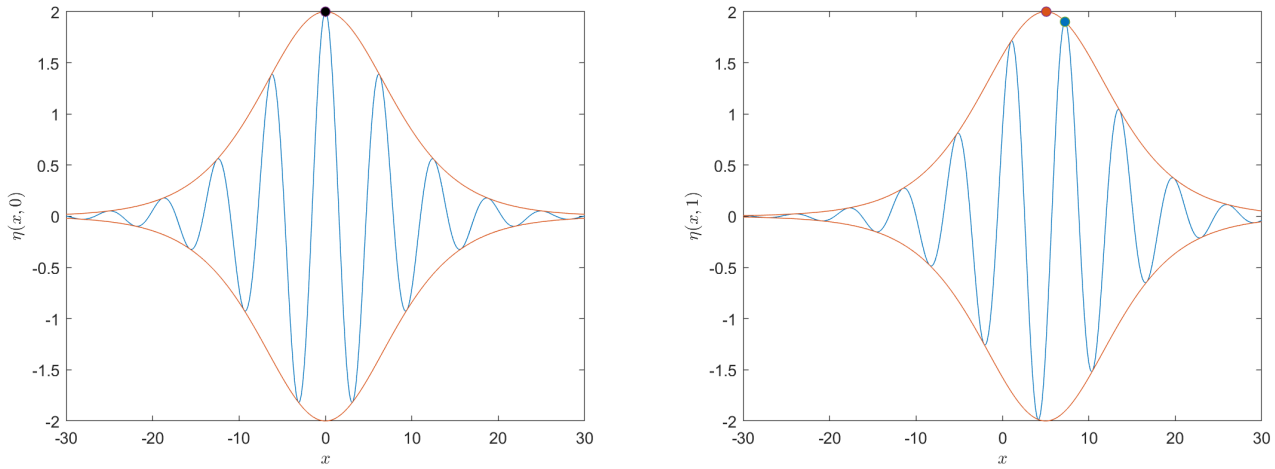

(a) (b)

Figure 1.5: Snapshots at $t = 0$ (a) and $t = 1$ (b) of (1.3.1)

Figure 1.5 gives an example of a non-linear wave-packet. The wave is given by

$$\eta(x,t) = 2\cos(x-t)\,\mathrm{sech}^2(0.1x - 0.5t) \tag{1.3.1}$$

so that it has the same phase speed and group velocity as the one in our previous example in Figure 1.4. To ascertain the validity of the last statement, we can check directly from the images. In both figures, the waves and the envelopes seem to have moved by the same amount in the same time interval.

In this frame of reference, the non-linear wave-packet cannot be time-periodic, as the envelope itself is not time-periodic and moves away from $x = 0$. This issue arises also when we try to find non-linear wave-packet solutions to our problem, but we will explain in the later sections how we deal with it.

1.3.1 Coriolis Platform

To ascertain the existence in real life of these nonlinear wave-packets, in 2009 Helfrich, Grimshaw and Johnson [6] performed a series of experiments at the LEGI-Coriolis Laboratory in Grenoble, which consisted in a tank with a rotating platform with diameter of 13 m and height of 8 m. This tank had two layers of water, where the lower one had salty water and the upper one had fresh water with depth 30 cm and 6 cm respectively. The rotation had a different frequency at each experiment which were given by $f = 0$, 0.105, 0.140, 0.209, $0.279 s^{-1}$.

In order to create the wave, a box of fresh water of width 5 m and length 45 cm was positioned near one of the walls of the tank. One could then manually let the water into the tank through a lock-release by the desirable amount.
For each set of probes, one of them is situated above the interface between salty and fresh water and one is positioned directly below, across the interface. The one above consists of a transmitter and a receiver, while the one below consists of a reflector. As the waves travel across the tank, the ultrasonic probes emit multiple signals per second which are reflected below the interface and eventually come back to the receiver. The probes then calculate the average time it took for the signals to come back by considering that sound speed travels faster through salty water, to figure out whether there was more fresh or salty water between the probes at that time. As the signals come back, the probes plot contours, which is exactly what is shown in Figure 1.6 (b). The blue colour indicates that there was more fresh water between the probes, while the red colour indicates that there was more salty water. From there we can therefore find the phase speed c_p by calculating the slope of lines parallel to bright red or strong blue stripes, and the group velocity c_g by considering the slope of lines on the right, where colours interchange. Here we obtained $c_p \approx 1.17$ and $c_g \approx 0.684$.

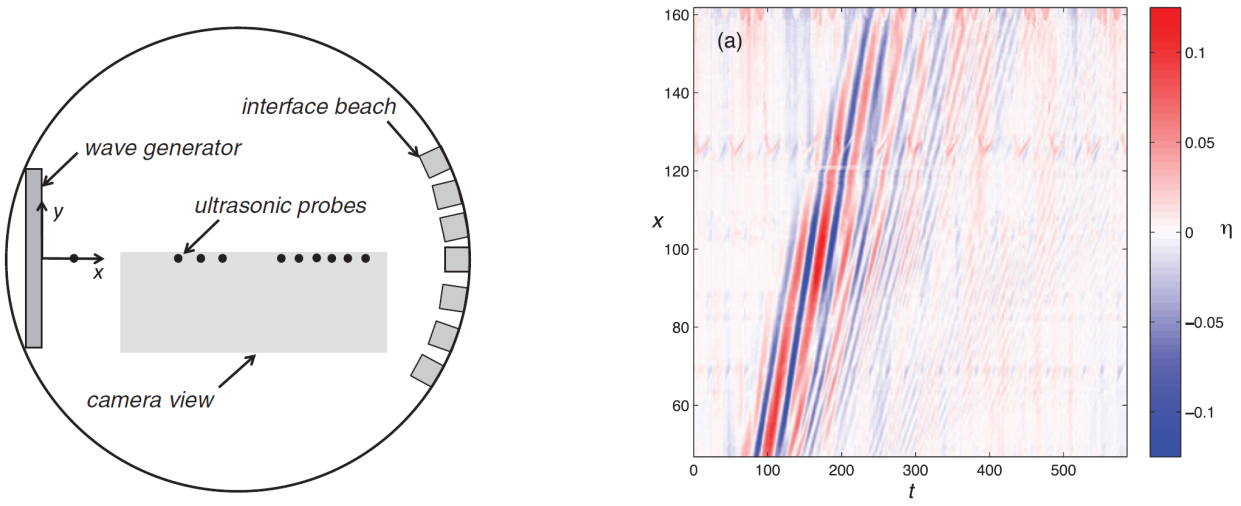

(a) (b)

Figure 1.6: Sketch from above of the Coriolis tank (a) and probes' measurements of nonlinear wave-packets (b) [6]

1.4 The Ostrovsky Equation

We will focus on finding solutions to the Ostrovsky equation:

$$(\eta_t + \nu\eta\eta_x + \beta\eta_{xxx})_x = \gamma\eta \tag{1.4.1}$$

where η represents the interfacial displacement, ν is the strength of weak nonlinearity, β is the weak hydrostatic dispersion and γ is a measure of the strength of weak rotation [15].

Ostrovsky first described this equation in 1978 [13] and it models weakly nonlinear internal waves in a rotating ocean, but removing the rotation leads to the well known Korteweg–De Vries (KdV) equation:

$$\eta_t + \nu\eta\eta_x + \beta\eta_{xxx} = 0 \tag{1.4.2}$$

For oceanic internal solitary waves, $\nu\beta > 0$ and $\gamma > 0$ so by introducing

$$x = L\tilde{x},\ t = T\tilde{t},\ \eta = M\tilde{\eta} \tag{1.4.3}$$

where $L^4 = \beta/\gamma,\ T = L^3/\beta,\ M = \beta/\nu L^2$, (1.1) becomes

$$(\tilde{\eta}_t + \tilde{\eta}\tilde{\eta}_x + \tilde{\eta}_{xxx})_x = \tilde{\eta} \tag{1.4.4}$$

Equation (1.4.4) is now parameter free and from now on, we will refer to it as the Ostrovsky equation after dropping the tildes.

1.4.1 Linear waves

We now look for a solution of the form

$$\eta(x,t) = e^{i(kx-\omega t)} \tag{1.4.5}$$

to establish a relation between the frequency ω, and the wave-number k, for linear wave solutions to the Ostrovsky equation.

Substituting (1.4.5) into (1.4.4) and neglecting the non-linear term gives:

$$(\omega k + k^4)e^{i(kx-\omega t)} = e^{i(kx-\omega t)} \tag{1.4.6}$$

which leads to

$$\omega = \frac{1}{k} - k^3 \tag{1.4.7}$$

From the frequency ω we can then find the phase speed c_p and the group velocity c_g of linear wave solutions to the Ostrovsky equation:

$$c_p = \frac{\omega}{k} = \frac{1}{k^2} - k^2, \; c_g = \frac{d\omega}{dk} = -3k^2 - \frac{1}{k^2} \tag{1.4.8}$$

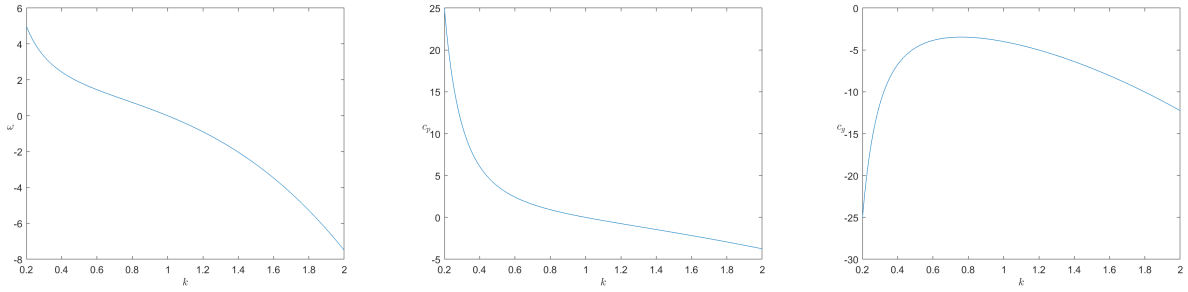

(a) (b) (c)

Figure 1.7: Frequency (a), phase speed (b) and group velocity (c) against k

The frequency ω and the phase speed c_p can take any value, while the group velocity c_g achieves its global maximum at $k = k_c = 3^{-1/4}$.

Chapter 2

The Nonlinear Schrödinger Theory

The Nonlinear Schrödinger (NLS) theory allows us to analyse nonlinear equations and find their solutions. Since it is known that the NLS theory works for the KdV equation [15], we expect that it will also work for our problem as the Ostrovsky equation is simply a rotational variant of the KdV.

2.1 The Nonlinear Schrödinger equation

The Nonlinear Schrödinger equation is given by

$$i(A_t + c_g A_x) + \Delta A_{xx} + \mu |A|^2 A = 0 \tag{2.1.1}$$

for the complex envelope $A(x,t)$ of the weakly nonlinear solution

$$\eta(x,t) = A(x,t)\exp(ikx - i\omega t) + \overline{A(x,t)\exp(ikx - i\omega t)} + \cdots \tag{2.1.2}$$

$$\eta(x,t) = A(x,t)\exp(ikx - i\omega t) + \overline{A(x,t)}\exp(i\omega t - ikx) + \cdots \tag{2.1.3}$$

where ω and k are the wave-number and frequency of the solution respectively, Δ is given by $\partial_k(c_g)/2$, with c_g being the group velocity of the solution and the constant μ depends on the type of equation we are solving. Here the bar denotes the complex conjugate and $|A| \ll 1$, while ∂_k represents the differential operator with respect to k [7].

2.2 The envelope of the solution

The introduction of the coordinates $X = x - c_g t$ and $T = t$ allows us to write with the aid of the Chain Rule the following

$$\frac{d}{dx} = \frac{\partial X}{\partial x}\frac{d}{dX} + \frac{\partial T}{\partial x}\frac{d}{dT} = \frac{d}{dX} \tag{2.2.1}$$

$$\frac{d}{dt} = \frac{\partial T}{dt}\frac{d}{dT} + \frac{dX}{dt}\frac{d}{dX} = \frac{d}{dT} - c_g\frac{d}{dX} \tag{2.2.2}$$

The NLS equation then becomes

$$i(A_T - c_g A_X + c_g A_X) + \Delta A_{XX} + \mu |A|^2 A = 0 \tag{2.2.3}$$

which is equivalent to

$$iA_T + \Delta A_{XX} + \mu |A|^2 A = 0 \tag{2.2.4}$$

We now look for a solution of the form

$$A(X,T) = F(X)\exp(-i\sigma T) \tag{2.2.5}$$

where F is a real valued function and σ is a real constant to be determined.
After Substituting (2.2.5) into (2.2.4), we obtain

$$i(-i\sigma)F\exp(-i\sigma T) + \Delta F^{''}\exp(-i\sigma T) + \mu F^2 F\exp(-i\sigma T) = 0 \tag{2.2.6}$$

Rearranging give us

$$(\sigma F + \Delta F^{''} + \mu F^3)\exp(-i\sigma T) = 0 \tag{2.2.7}$$

Since the equation must hold for all T, we have that

$$\sigma F + \Delta F^{''} + \mu F^3 = 0 \tag{2.2.8}$$

Try

$$F(X) = a\,\mathrm{sech}(KX) \tag{2.2.9}$$

where $a \ll 1$ and K is another real constant.
We note that using the following hyperbolic trigonometric identity

$$\mathrm{sech}^2(x) + \tanh^2(x) = 1 \tag{2.2.10}$$

we obtain

$$F'(X) = -aK\,\mathrm{sech}(KX)\tanh(KX) \tag{2.2.11}$$

$$\begin{aligned} F''(X) &= aK^2\,\mathrm{sech}(KX)\tanh^2(KX) - aK^2\,\mathrm{sech}^3(KX) \\ &= aK^2\,\mathrm{sech}(KX)(\tanh^2(KX) - \mathrm{sech}^2(KX)) \\ &= aK^2\,\mathrm{sech}(KX)(1 - 2\,\mathrm{sech}^2(KX)) \\ &= aK^2\,\mathrm{sech}(KX) - 2aK^2\,\mathrm{sech}^3(KX) \end{aligned} \tag{2.2.12}$$

Hence (2.2.8) becomes

$$\begin{aligned} 0 &= \sigma a\,\mathrm{sech}(KX) + \Delta aK^2\,\mathrm{sech}(KX) - 2\Delta aK^2\,\mathrm{sech}^3(KX) + \mu a^3\,\mathrm{sech}^3(KX) \\ &= (\sigma + \Delta K^2)\,\mathrm{sech}(KX) + (\mu a^2 - 2\Delta K^2)\,\mathrm{sech}^3(KX) \end{aligned} \tag{2.2.13}$$

and if we choose σ and K in a way such that

$$\sigma + \Delta K^2 = 0 \tag{2.2.14}$$

$$\mu a^2 - 2\Delta K^2 = 0 \tag{2.2.15}$$

we can obtain a solution that satisfies the NLS equation, which would be given by

$$A(x,t) = a\,\mathrm{sech}[K(x - c_g t)]\exp(-i\sigma t) \tag{2.2.16}$$

$$K = a\left(\frac{\mu}{2\Delta}\right)^{\frac{1}{2}}, \quad \sigma = -\frac{\mu a^2}{2}, \quad a \ll 1 \tag{2.2.17}$$

So, in order to solve the Ostrovsky equation, we need to find a way to relate it with the NLS equation.

2.3 Derivation of the NLS equation from the Ostrovsky equation

Professor R.S. Johnson introduced a method that allowed him to recover the NLS equation from various non-linear equations like the KdV equation [8], but for our problem, we will use this method to recover the NLS equation from the Ostrovsky equation.

Recall the Ostrovsky equation

$$(\eta_t + \eta\eta_x + \eta_{xxx})_x = \eta \tag{2.3.1}$$

$$\iff \eta_{tx} + \frac{1}{2}\left(\eta^2\right)_{xx} + \eta_{xxxx} = \eta \tag{2.3.2}$$

We look for small-amplitude solutions, so that $\eta = \epsilon\eta_0$ where $\epsilon \ll 1$. Then (2.3.2) becomes

$$\epsilon\eta_{0tx} + \frac{\epsilon^2}{2}(\eta_0^2)_{xx} + \epsilon\eta_{0xxxx} = \epsilon\eta_0 \tag{2.3.3}$$

Let's now make a change of coordinates by introducing $\hat{t} = \epsilon t$. We then obtain

$$\epsilon^2\eta_{0\hat{t}x} + \frac{\epsilon^2}{2}(\eta_0^2)_{xx} + \epsilon\eta_{0xxxx} = \epsilon\eta_0 \tag{2.3.4}$$

or

$$\eta_{0\hat{t}x} + \frac{1}{2}(\eta_0^2)_{xx} + \lambda\eta_{0xxxx} = \lambda\eta_0 \tag{2.3.5}$$

where $\lambda = \epsilon^{-1}$.
We further introduce the following set of coordinates

$$\begin{aligned} X &= \lambda^{-1}(x - \lambda c_{g_1}\hat{t}) \\ Z &= x - \lambda c_{p_1}\hat{t} \ \ (= x - c_p t) \\ T &= \lambda^{-1}\hat{t} \end{aligned} \tag{2.3.6}$$

where c_{p_1} and c_{g_1} are approximations for the phase speed and the group velocity respectively. From (2.3.6) we obtain

$$\begin{aligned} \frac{\partial}{\partial x} &= \frac{\partial X}{\partial x}\frac{\partial}{\partial X} + \frac{\partial Z}{\partial x}\frac{\partial}{\partial Z} + \frac{\partial T}{\partial x}\frac{\partial}{\partial T} \\ &= \lambda^{-1}\frac{\partial}{\partial X} + \frac{\partial}{\partial Z} \end{aligned} \tag{2.3.7}$$

$$\begin{aligned} \frac{\partial}{\partial t} &= \frac{\partial T}{\partial t}\frac{\partial}{\partial T} + \frac{\partial X}{\partial t}\frac{\partial}{\partial X} + \frac{\partial Z}{\partial t}\frac{\partial}{\partial Z} \\ &= \lambda^{-1}\frac{\partial}{\partial T} - c_{g_1}\frac{\partial}{\partial X} - \lambda c_{p_1}\frac{\partial}{\partial Z} \end{aligned} \tag{2.3.8}$$

After substituting (2.3.7) and (2.3.8) into (2.3.5), the Ostrovsky equation then becomes

$$\begin{aligned} (\lambda^{-2}\eta_{0TX} + \lambda^{-1}\eta_{0TZ} - \lambda c_{p_1}\eta_{0ZZ} - c_{g_1}\lambda^{-1}\eta_{0XX} - (c_{g_1} + c_{p_1})\eta_{0XZ}) + \frac{1}{2}\left[(\eta_0^2)_{ZZ} + 2\lambda^{-1}(\eta_0^2)_{XZ} + \lambda^{-2}(\eta_0^2)_{XX}\right] \\ + \lambda(\lambda^{-4}\eta_{0XXXX} + 4\lambda^{-3}\eta_{0XXXZ} + 6\lambda^{-2}\eta_{0XXZZ} + 4\lambda^{-1}\eta_{0XZZZ} + \eta_{0ZZZZ}) = \lambda\eta_0 \end{aligned} \tag{2.3.9}$$

and we write the solution as an expansion in powers of $\lambda^{-1} = \epsilon$

$$\eta_0 = \sum_{n=0}^{\infty} \lambda^{-n} \left\{ \sum_{m=0}^{n+1} A_{nm}(X,T)E^m + \text{c.c} \right\} \tag{2.3.10}$$

where $E = \exp(ikZ)$, c.c denotes the complex conjugate of $A_{nm}(X,T)E^m$ for $m \geq 1$, and $A_{00} = 0$. Here k gives the wave-number of our solution.

At order λE we have

$$\begin{aligned} -c_{p_1}A_{01}(ik)^2 + A_{01}(ik)^4 &= A_{01} \\ k^2 c_{p_1} + k^4 &= 1 \end{aligned} \tag{2.3.11}$$

for $A_{01} \neq 0$, which leads to

$$c_{p_1} = \frac{1}{k^2} - k^2 \tag{2.3.12}$$

This value is the same as the phase speed of the linear waves that we found in Section 1.4.1, and hence that value is a good approximation for the phase speed of nonlinear wave-packet solutions to the Ostrovsky equation.
We therefore set $c_{p_1} := c_p$.

We now look for terms at order E

$$-c_p A_{11}(ik)^2 + A_{11}(ik)^4 - (c_{g_1} + c_p)A_{01X}(ik) + 4(ik)^3 A_{01X} = A_{11} \tag{2.3.13}$$

$$\iff (k^2 c_p + k^4 - 1)A_{11} = i[k(c_{g_1} + c_p) + 4k^3]A_{01X} \tag{2.3.14}$$

But by (2.3.11), $k^2 c_p + k^4 - 1 = 0$ and therefore, assuming that $A_{01X} \neq 0$

$$k(c_{g_1} + c_p) + 4k^3 = 0 \tag{2.3.15}$$

ultimately obtaining that

$$c_{g_1} = -\frac{1}{k^2} - 3k^2 \tag{2.3.16}$$

Again, this is the same as the value we obtained in Section 1.3.1. We therefore conclude that the group velocity of linear wave solutions to the Ostrovsky equation, approximates well the one for non-linear wave solutions, and we set $c_{g_1} := c_g$.

At order E^2, (2.3.9) gives

$$-c_p A_{12}(2ik)^2 + \frac{1}{2}A_{01}^2(2ik)^2 + A_{12}(2ik)^4 = A_{12} \tag{2.3.17}$$

After rearranging we obtain

$$\begin{aligned} A_{12} &= \frac{2k^2}{16k^4 + 4k^2 c_p - 1} A_{01}^2 \\ &= \frac{2k^2}{12k^4 + 3} A_{01}^2 \end{aligned} \tag{2.3.18}$$

This result will be useful for the next part.

Next, at order $\lambda^{-1}E$ we have

$$\begin{aligned} (ik)A_{01T} - c_p A_{21}(ik)^2 - c_g A_{01XX} - (c_g + c_p)A_{11X}(ik) + A_{12}\overline{A_{01}}(ik)^2 \\ + 6A_{01XX}(ik)^2 + 4A_{11X}(ik)^3 + A_{21}(ik)^4 = A_{21} \end{aligned} \tag{2.3.19}$$

$$\begin{aligned} \iff & ikA_{01T} - (c_g + 6k^2)A_{01XX} - k^2 A_{12}\overline{A_{01}} \\ & + (k^2 c_p + k^4 - 1)A_{21} - i[k(c_g + c_p) + 4k^3]A_{11X} = 0 \end{aligned} \tag{2.3.20}$$

We may now substitute (2.3.18) into (2.3.20). At the same time we note that $k^2 c_p + k^4 - 1 = 0$ and $k(c_g + c_p) + 4k^3 = 0$ by (2.3.11) and (2.3.15) respectively. Hence (2.3.20) becomes

$$iA_{01T} + \left(\frac{1}{k^3} - 3k\right)A_{01XX} - \frac{2k^3}{12k^4 + 3}A_{01}|A_{01}|^2 = 0 \tag{2.3.21}$$

Notice that

$$\frac{\partial c_g}{\partial k} = \frac{2}{k^3} - 6k \tag{2.3.22}$$

So we may therefore write equation (2.3.21) as

$$iA_{01T} + \frac{1}{2}\frac{\partial c_g}{\partial k}A_{01XX} - \frac{2k^3}{12k^4 + 3}A_{01}|A_{01}|^2 = 0 \tag{2.3.23}$$

which has the same form of (2.2.4).
Let's find the first terms in the expansion of (2.3.10). We have

$$\begin{aligned} \eta_0 &= A_{01}\exp(ikZ) + \overline{A_{01}}\exp(-ikZ)\cdots \\ &= A_{01}\exp(ikx - ikc_p t) + \overline{A_{01}}\exp(ikc_p t - ikx) + \cdots \\ &= A_{01}\exp(ikx - i\omega t) + \overline{A_{01}}\exp(i\omega t - ikx) + \cdots \end{aligned} \tag{2.3.24}$$

as $Z = x - c_p t$ and $c_p = \omega/k$.
But since $\eta = \epsilon\eta_0$, when we compare (2.3.24) with (2.1.3), we can see that $\epsilon A_{01} = A$. At the same time, we found a set of coordinates for which A_{01} satisfies the NLS equation (2.2.4) with

$$\Delta = \frac{1}{2}\frac{\partial c_g}{\partial k} \quad \text{and} \quad \mu = -\frac{2k^3}{12k^4 + 3} \tag{2.3.25}$$

and therefore, by (2.2.16) and (2.2.17) we have that

$$\begin{aligned} \epsilon A_{01}(x,t) = A(x,t) &= a\,\mathrm{sech}[K(x - c_g t)]\exp(-i\sigma t) \\ K = a\left(\frac{\mu}{2\Delta}\right)^{\frac{1}{2}}, &\quad \sigma = -\frac{\mu a^2}{2}, \quad a = \epsilon \ll 1 \end{aligned} \tag{2.3.26}$$

with Δ and μ given by (2.3.25).

But in order to have real solutions, we would need that K remained real. This happens when

$$\frac{\mu}{2\Delta} = \frac{k^6}{36k^8 - 3k^4 - 3} > 0 \tag{2.3.27}$$

Hence we need to find the values of $k > 0$ for which (2.3.27) is true.

Now, since $k^6 > 0$ for all $k > 0$, we only need to solve

$$36k^8 - 3k^4 - 3 > 0 \tag{2.3.28}$$

To solve the above we start by finding the real roots of $p(k) = 36k^8 - 3k^4 - 3$, which is quadratic in k^4. We obtain

$$\begin{aligned} k^4 &= \frac{1 \pm \sqrt{1+48}}{24} \\ &= \frac{1 \pm 7}{24} \end{aligned} \tag{2.3.29}$$

We ignore complex roots, hence

$$k^4 = \frac{1}{3} \Rightarrow k^2 = \pm\frac{1}{\sqrt{3}} \tag{2.3.30}$$

Again, ignoring complex roots, we find that

$$k = \pm\frac{1}{\sqrt[4]{3}} \tag{2.3.31}$$

But since we require that $k > 0$, real solutions are achieved when

$$k > \frac{1}{\sqrt[4]{3}} \tag{2.3.32}$$

Chapter 3

Numerical Results

In this section we will describe how we computed numerical computations of solutions to the Ostrovsky equation. We will integrate the equation in Fourier Space which reduces the PDE to an ODE, with the aid of the 4th Order Runge-Kutta Method.

3.1 Time-periodic Solutions

Our interest lies in time-periodic solutions, but finding these manually can prove to be difficult. We know the envelope of our solution moves with speed c_g, so if we integrated the equation in the frame of reference of the envelope, our solution would then be time-periodic. In order to this, we introduce the coordinates

$$\tilde{x} = x - c_g t \quad \text{and} \quad \tilde{t} = t \tag{3.1.1}$$

like we did in Section 2. The Ostrovsky equation then becomes

$$(\eta_{\tilde{t}} - c_g \eta_{\tilde{x}} + \eta\eta_{\tilde{x}} + \eta_{\tilde{x}\tilde{x}\tilde{x}})_{\tilde{x}} = \eta \tag{3.1.2}$$

After dropping the tildes, we will refer to the above as the Modified Ostrovsky equation.

To show the effect of the new coordinates, we will use them in the example that we described in Section 1.2, where

$$\eta(x,t) = 2\cos(x-t)\cos(0.1x - 0.5t), \ c_g = 5 \tag{3.1.3}$$

Substituting (3.1.1) into (3.1.3) gives

$$\eta(\tilde{x},\tilde{t}) = 2\cos(\tilde{x} + 4\tilde{t})\cos(0.1\tilde{x}) \tag{3.1.4}$$

Figure 3.1 shows exactly what we wanted to describe. In (b), the red dot has remained stationary meaning that the envelope of the wave is steady, while the wave itself keeps propagating within the envelope, as the blue dot has moved. Under this change of coordinates, the wave can now be time-periodic with period $T = \pi/2$, and it completes a full period when the peak on the left of the blue dot arrives at the red dot.

3.2 Stability of the 4th order Runge-Kutta Method

Consider an ODE formulation of the form

$$\begin{aligned} &\frac{\mathrm{d}y}{\mathrm{d}t} = f(y,t), \\ &y(0) = y_0, \quad 0 \le t \le T \end{aligned} \tag{3.2.1}$$

and suppose that a finite difference method for the numerical integration of the above was given by

$$y_{n+1} = Y(y_n, t_n) \tag{3.2.2}$$

where the time-step taken for discretisation was $\mathrm{d}t$, so that $t_n = n\mathrm{d}t$, $n = 0, 1, 2, \ldots, N$, and y_n is the numerical approximation of $y(t_n)$.

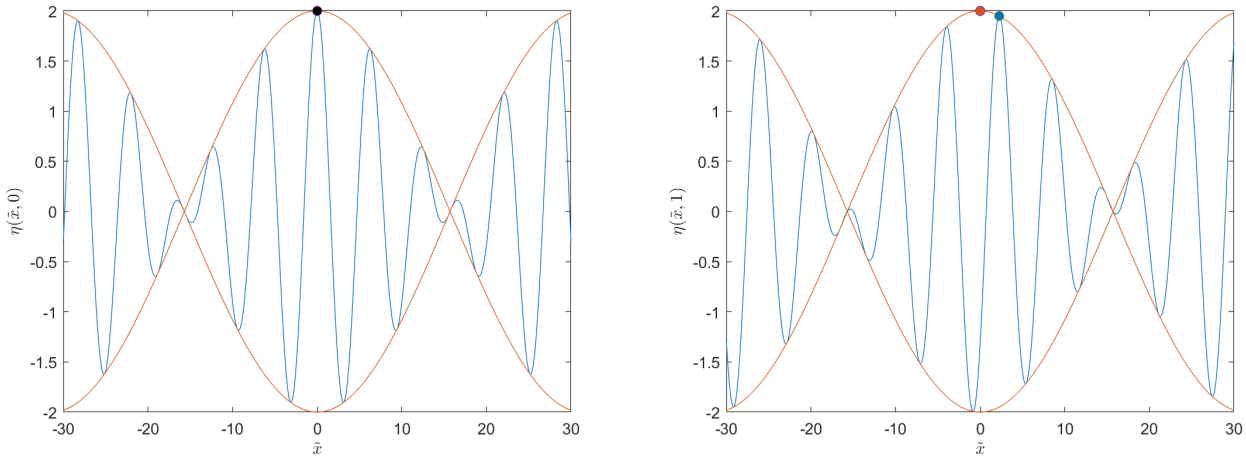

(a) (b)

Figure 3.1: Snapshots at $t = 0$ (a) and $t = 1$ (b) of (3.1.4)

Let's now perturb y_n by some small amount ϵ_n. Hence the perturbation in y_{n+1} will be ϵ_{n+1} and

$$y_{n+1} + \epsilon_{n+1} = Y(y_n + \epsilon_n, t_n) \tag{3.2.3}$$

Taylor expanding $Y(y_n + \epsilon_n, t_n)$ around (y_n, t_n) gives

$$y_{n+1} + \epsilon_{n+1} = Y(y_n, t_n) + \epsilon_n \frac{\partial Y(y_n, t_n)}{\partial y_n} + O(\epsilon_n^2) \tag{3.2.4}$$

After neglecting terms smaller than ϵ_n in size we obtain

$$\epsilon_{n+1} = \frac{\partial y_{n+1}}{\partial y_n} \epsilon_n \tag{3.2.5}$$

or better

$$\epsilon_n = \left(\frac{\partial y_{n+1}}{\partial y_n} \right)^n \epsilon_0 \tag{3.2.6}$$

and we have stability when

$$|g_n| = \left| \frac{\partial y_{n+1}}{\partial y_n} \right| < 1 \tag{3.2.7}$$

If $|g_n| = 1$ then the algorithm is neutrally stable. Otherwise we just say that the method is unstable to perturbations, and numerical solutions tend to grow in size with increasing n. Later we will show that solutions to the Ostrovsky equation are bounded, and we will therefore require that the finite difference method that we use satisfies the above stability condition.

Now, the 4th Order Runge-Kutta Method is given by

$$\begin{aligned} k_1 &= \mathrm{d}t \; f(y_n, t_n) \\ k_2 &= \mathrm{d}t \; f\left(y_n + \frac{k_1}{2}, t_n + \frac{\mathrm{d}t}{2} \right) \\ k_3 &= \mathrm{d}t \; f\left(y_n + \frac{k_2}{2}, t_n + \frac{\mathrm{d}t}{2} \right) \\ k_4 &= \mathrm{d}t \; f(y_n + k_3, t_n + \mathrm{d}t) \end{aligned} \tag{3.2.8}$$

$$y_{n+1} = y_n + \frac{1}{6}(k_1 + 2k_2 + 2k - 3 + k_4) \tag{3.2.9}$$

and suppose that $f(y,t) = \lambda y$ where $\lambda < 0$. Then

$$y_{n+1} = y_n(1 + \mathrm{d}t\lambda + \frac{1}{2}(\mathrm{d}t\lambda)^2 + \frac{1}{6}(\mathrm{d}t\lambda)^3 + \frac{1}{24}(\mathrm{d}t\lambda)^4) \tag{3.2.10}$$

and we obtain stability when

$$\left|\frac{\partial y_{n+1}}{\partial y_n}\right| = |1 + \mathrm{d}t\lambda + \frac{1}{2}(\mathrm{d}t\lambda)^2 + \frac{1}{6}(\mathrm{d}t\lambda)^3 + \frac{1}{24}(\mathrm{d}t\lambda)^4| < 1 \tag{3.2.11}$$

Define

$$g(x) = 1 + x + \frac{x^2}{2} + \frac{x^3}{6} + \frac{x^4}{24} \tag{3.2.12}$$

and by using the online software GeoGebra we can find the values of x for which $|g(x)| < 1$.

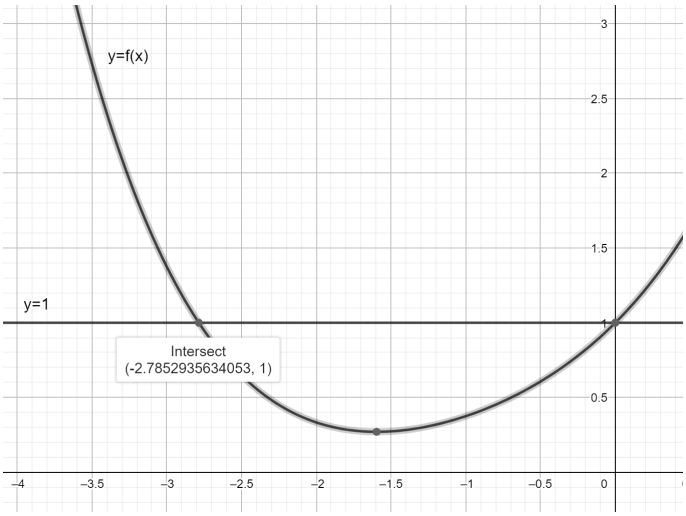

Figure 3.2: Graph of $|g(x)|$

So we see that approximately, x needs to satisfy $-2.785 < x < 0$ or in our case $-2.785 < \mathrm{d}t\lambda < 0$. The right inequality is already satisfied since $\lambda < 0$ so our result leads to

$$\mathrm{d}t < \frac{2.785}{|\lambda|} \tag{3.2.13}$$

The exact solution to the ODE formulation is given by

$$y(t) = y_0 e^{\lambda t} \tag{3.2.14}$$

Now consider the case when $\lambda > 0$. Then the above grows exponentially. From (3.2.10), one can write

$$y_n = (1 + \mathrm{d}t\lambda + \frac{1}{2}(\mathrm{d}t\lambda)^2 + \frac{1}{6}(\mathrm{d}t\lambda)^3 + \frac{1}{24}(\mathrm{d}t\lambda)^4)^n y_0 \tag{3.2.15}$$

Here y_n also grows as n increases but not exponentially, and therefore we are not interested in the stability of the algorithm. The error in the approximation arises only due to the difference in the growth rate as time increases.

Suppose now that λ was purely imaginary so that $\mathrm{d}t\lambda = iw$, where w is real valued. Then from (3.2.15) we have that

$$\begin{aligned} |1 + iw + \frac{1}{2}(iw)^2 + \frac{1}{6}(iw)^3 + \frac{1}{24}(iw)^4| &< 1 \\ |(1 - \frac{w^2}{2} + \frac{w^4}{24}) + i(w - \frac{w^3}{6})| &< 1 \\ (1 - \frac{w^2}{2} + \frac{w^4}{24})^2 + (w - \frac{w^3}{6})^2 &< 1 \end{aligned} \tag{3.2.16}$$

which reduces to

$$w^6(w^2 - 8) < 0 \tag{3.2.17}$$

Therefore we obtain that

$$0 < \frac{\mathrm{d}t\lambda}{i} < \sqrt{8} \quad \text{or} \quad -\sqrt{8} < \frac{\mathrm{d}t\lambda}{i} < 0 \tag{3.2.18}$$

which leads to

$$\mathrm{d}t < \frac{\sqrt{8}}{|\lambda|} \tag{3.2.19}$$

3.3 Stiffness

Suppose we wanted to numerically compute the solutions to the following ODEs

$$\frac{\mathrm{d}u}{\mathrm{d}t} = -200u \tag{3.3.1}$$

$$\frac{\mathrm{d}v}{\mathrm{d}t} = -0.03v \tag{3.3.2}$$

From the previous section, we know that in order to achieve stability we require $\mathrm{d}t < 2.785/200 = 0.0138$ for the first ODE, and $\mathrm{d}t < 2.785/0.03 = 91.7$ for the second ODE. If we wanted to use the same time-step for both integrations, we therefore would need that $\mathrm{d}t < 0.0138$. But since the second ODE does not require such small time-step to reach stability, computing its solution would be numerically wasteful. If for instance we wanted to compute the solution to (3.21) for $0 \leq t \leq 10$ using a time-step satisfying the inequality we just found, we would need at least 724 iterations, while $\mathrm{d}t = 0.5 < 91.7$ would require only 20 iterations. This is known as stiffness and we will encounter it as we try integrating the Ostrosky equation.

3.4 Integrating factor Method

We shall now apply the Fourier Transform to the Modified Ostrovsky equation to reduce the problem from a PDE to an ODE.

We start by writing the Modified Ostrovsky equation in the following form

$$\eta_{tx} - c_g\eta_{xx} + \frac{1}{2}(\eta^2)_{xx} + \eta_{xxxx} = \eta \tag{3.4.1}$$

We then apply the Fourier Transform to the above to obtain

$$\begin{aligned} &(i\xi)\left(\hat{\eta}_t - (i\xi)c_g\hat{\eta} + \frac{1}{2}(i\xi)\widehat{\eta^2} + (i\xi)^3\hat{\eta}\right) = \hat{\eta} \\ &\hat{\eta}_t + \frac{i}{2}\xi\widehat{\eta^2} - i\Gamma\hat{\eta} = 0 \end{aligned} \tag{3.4.2}$$

where $\Gamma(\xi) = c_g\xi + \xi^3 - 1/\xi$, $\hat{\eta}(\xi, t) = \mathcal{F}(\eta(x, t))$ denotes the Fourier Transform of η and

$$\mathcal{F}\left(\frac{\partial^n}{\partial x^n}\left(f(x, t)\right)\right) = (i\xi)^n\hat{f}(\xi, t) \tag{3.4.3}$$

for any smooth function f and any positive integer n.
For now, let's neglect the non-linear term and suppose we wanted to solve

$$\hat{\eta}_t = i\Gamma\hat{\eta} \tag{3.4.4}$$

Because we applied the Fourier Transform with respect to x, we can think of ξ as a variable that represents all the possible wave-numbers for our solution. If we discretise the problem in ξ we obtain the following system of ODEs

$$\begin{aligned} \hat{\eta}_t(\xi_1) &= i\Gamma(\xi_1)\hat{\eta}(\xi_1) \\ \hat{\eta}_t(\xi_2) &= i\Gamma(\xi_2)\hat{\eta}(\xi_2) \\ &\vdots \\ \hat{\eta}_t(\xi_N) &= i\Gamma(\xi_N)\hat{\eta}(\xi_N) \end{aligned} \tag{3.4.5}$$

and since $i\Gamma(\xi_j)$ is purely imaginary for each $j = 1, 2, \ldots, N$, our time-step $\mathrm{d}t$ would have to satisfy

$$\mathrm{d}t < \frac{\sqrt{8}}{\lambda_{\max}} \tag{3.4.6}$$

where $\lambda_{\max} = \max_{j=1,\ldots,N} |i\Gamma(\xi_j)|$.

But if ξ_j is large in magnitude for some j, then so is $i\Gamma$. Similarly happens if ξ_j is really small in magnitude, due to the $1/\xi$ term in Γ. We would therefore need a really small time-step in order to obtain stability. But at the same time, we cannot exclude the possibility that we have some ξ_j for which $|i\Gamma|$ is not as large. This unfortunately creates a stiff problem. In order to circumvent this, we introduce an integrating factor similar to the one Prof. LLoyd N. Trefethen [14] did when he numerically integrated the KdV equation, to transform the Modified Ostrovsky equation into one where we don't have to consider linear terms.
We now multiply (3.4.2) by $e^{-i\Gamma t}$ to get

$$\hat{\eta}_t e^{-i\Gamma t} + \frac{i}{2}\xi\widehat{\eta^2}e^{-i\Gamma t} - i\Gamma\hat{\eta}e^{-i\Gamma t} = 0 \tag{3.4.7}$$

By introducing the following quantity

$$\hat{\mathrm{H}} = \hat{\eta}e^{-i\Gamma t} \tag{3.4.8}$$

where

$$\hat{\mathrm{H}}_t = \hat{\eta}_t e^{-i\Gamma t} - i\Gamma\hat{\eta}e^{-i\Gamma t} \tag{3.4.9}$$

we obtain

$$\hat{\mathrm{H}}_t + \frac{i}{2}\xi\widehat{\eta^2}e^{-i\Gamma t} = 0 \tag{3.4.10}$$

which does not contain any linear terms, as required.

For computation purposes, it is better to write (3.4.10) as follows

$$\hat{\mathrm{H}}_t = -\frac{i}{2}\xi\mathcal{F}((\mathcal{F}^{-1}(\hat{\mathrm{H}}e^{i\Gamma t}))^2)e^{-i\Gamma t} \tag{3.4.11}$$

so that we may perform the integration with time for $\hat{\mathrm{H}}$. We may then recover η using (3.4.8).

3.5 Boundedness of the solution

Suppose the solution to the Ostrovsky equation $\eta(x,t)$ is continuously differentiable on the interval $[-L, L]$ for $t \geq 0$, and that η, its derivatives and anti-derivatives with respect of x take the same value at $x = \pm L$. We need to make sure that if the solution is bounded at $t = 0$, then it should also be bounded for $t > 0$, or else, the solution would diverge and numerical integration would not work.

Let $g(x,t)$ be an anti-derivative of $\eta(x,t)$ with respect of x so that

$$\frac{\partial}{\partial x}(g(x,t)) = \eta(x,t) \tag{3.5.1}$$

We can then write the Ostrovsky equation as

$$\eta_t = -\eta\eta_x - \eta_{xxx} + g(x,t) \tag{3.5.2}$$

Let's now multiply both sided of the above equation by η to obtain

$$\eta\eta_t = -\eta^2\eta_x - \eta\eta_{xxx} + \eta g(x,t) \tag{3.5.3}$$

We notice that

$$\eta\eta_t = \frac{1}{2}\frac{\partial}{\partial t}(\eta^2) \tag{3.5.4}$$

$$\eta^2\eta_t = \frac{1}{3}\frac{\partial}{\partial x}(\eta^3) \tag{3.5.5}$$

$$\eta g(x,t) = \frac{1}{2}\frac{\partial}{\partial x}(g(x,t)^2) \tag{3.5.6}$$

Substituting these into (3.11) and integrating from $-L$ to L with respect to x gives

$$\begin{aligned}\frac{1}{2}\frac{\partial}{\partial t}\int_{-L}^{L}\eta^2\ \mathrm{d}x &= \int_{-L}^{L}\left(-\frac{1}{3}\frac{\partial}{\partial x}(\eta^3) - \eta\eta_{xxx} + \frac{1}{2}\frac{\partial}{\partial x}(g(x,t)^2)\right)\mathrm{d}x \\ &= \int_{-L}^{L}\frac{\partial}{\partial x}\left(\frac{1}{2}g^2 - \frac{1}{3}\eta^3\right)\mathrm{d}x - \int_{-L}^{L}\eta\eta_{xxx}\ \mathrm{d}x\end{aligned} \tag{3.5.7}$$

By the Fundamental Theorem of Calculus we have that

$$\int_{-L}^{L}\frac{\partial}{\partial x}\left(\frac{1}{2}g^2 - \frac{1}{3}\eta^3\right)\mathrm{d}x = \frac{1}{2}(g(L,t)^2 - g(-L,t)^2) - \frac{1}{3}(\eta(L,t)^3 - \eta(-L,t)^3) \tag{3.5.8}$$

but by our assumption, $g(L,t) = g(-L,t)$ and $\eta(L,t) = \eta(-L,t)$, so the right-hand-side of (3.17) vanishes.

The only term remaining gives

$$\begin{aligned}\int_{-L}^{L}\eta\eta_{xxx}\ \mathrm{d}x &= \int_{-L}^{L}\eta_x\eta_{xx}\mathrm{d}x - [\eta\eta_{xx}]_L^L \\ &= \frac{1}{2}\int_{-L}^{L}\frac{\partial}{\partial x}(\eta_x^2)\mathrm{d}x \\ &= \frac{1}{2}(\eta_x(L,t)^2 - \eta_x(-L,t)^2) \\ &= 0\end{aligned} \tag{3.5.9}$$

since we know that η and its derivatives take the same value at the boundaries of the x-domain.

So we have proved that

$$\frac{\partial}{\partial t}\int_{-L}^{L}\eta^2\ \mathrm{d}x = 0 \tag{3.5.10}$$

or

$$\int_{-L}^{L}\eta^2\ \mathrm{d}x = C \tag{3.5.11}$$

where C is a constant.

This quantity is known as the momentum flux of the wave and by showing that it is a constant at all times, we have proved that the solution is bounded for all $t \geq 0$.

A good way to check this numerically can be captured by Parseval's Theorem, as it allows us to make a connection between the momentum flux and the Fourier coefficients of the solution. It states that if

$$\eta(x,t) = c(t) + \sum_{n=1}^{\infty}\left(a_n(t)\cos\left(\frac{n\pi x}{L}\right) + b_n(t)\sin\left(\frac{n\pi x}{L}\right)\right) \tag{3.5.12}$$

where $c(t)$, $a_n(t)$ and $b_n(t)$ represent the Fourier coefficients of η at time t. Then

$$\frac{1}{L}\int_{-L}^{L}\eta^2\ \mathrm{d}x = 2c(t)^2 + \sum_{n=1}^{\infty}(a_n(t)^2 + b_n(t)^2) = \frac{C}{L} \tag{3.5.13}$$

This enables us to check the validity of our solution: if the Fourier coefficients of our solution satisfy (3.8) before and after the integration in time, then it implies that that solution is a valid one. In our computations our solutions satisfied this condition with an error of 10^{-4}, which can be attributed to the performance of the program.

3.6 The initial guess

In order to perform integration in time we obviously require an initial guess. We will use the solution found in Section 2 of the form

$$\eta(x,t) = A(x,t)\exp(ikx - i\omega t) + \overline{A(x,t)}\exp(i\omega t - ikx) \tag{3.6.1}$$

where ω and k are as usual the frequency and the wave-number of the wave-packet, and the complex envelope $A(x,t)$ was given by

$$A(x,t) = a\,\mathrm{sech}[K(x - c_g t)]\exp(-i\sigma t) \tag{3.6.2}$$

where

$$K = a\left(\frac{\mu}{2\Delta}\right)^{\frac{1}{2}}, \quad \sigma = -\frac{\mu a^2}{2} \tag{3.6.3}$$

with

$$\Delta = \frac{1}{2}\frac{\partial c_g}{\partial k}, \quad \mu = -\frac{2k^3}{12k^4 + 3} \tag{3.6.4}$$

Clearing everything up, we obtain

$$\eta(x,t) = 2a\,\mathrm{sech}[K(x - c_g t)]\cos[kx - (\omega + \sigma)t] \tag{3.6.5}$$

with all of the constants given above.

To establish approximately valid values of a and k, we will refer to the analysis made by A.J. Whitfield and E.R. Johnson [15]. From Figure 3.3, we pick a maximum value for η defined via $\eta_{\max} = 2a$ and find the corresponding value for a_s. We then choose a k from Figure 3.4 which matches with the previously found value of a_s. The value a_s comes from the initial conditions used by the authors of the analysis to perform integration in time. They were of the form

$$\eta(x,0) = a_s\,\mathrm{sech}^2(x/D) \quad \text{where} \quad D^2 = \frac{12}{a_s} \tag{3.6.6}$$

The value a_s is not relevant and therefore not helpful for our aim, as this analysis was performed using solitons as initial conditions (see Figure 3.5), while our interest lies in wave-packets. Because our theory is valid only for $a \ll 1$, for our initial guess we took $a = 1/2$, which lead us to obtain $k \approx 0.97$ and $c_g =\approx -3.89$.

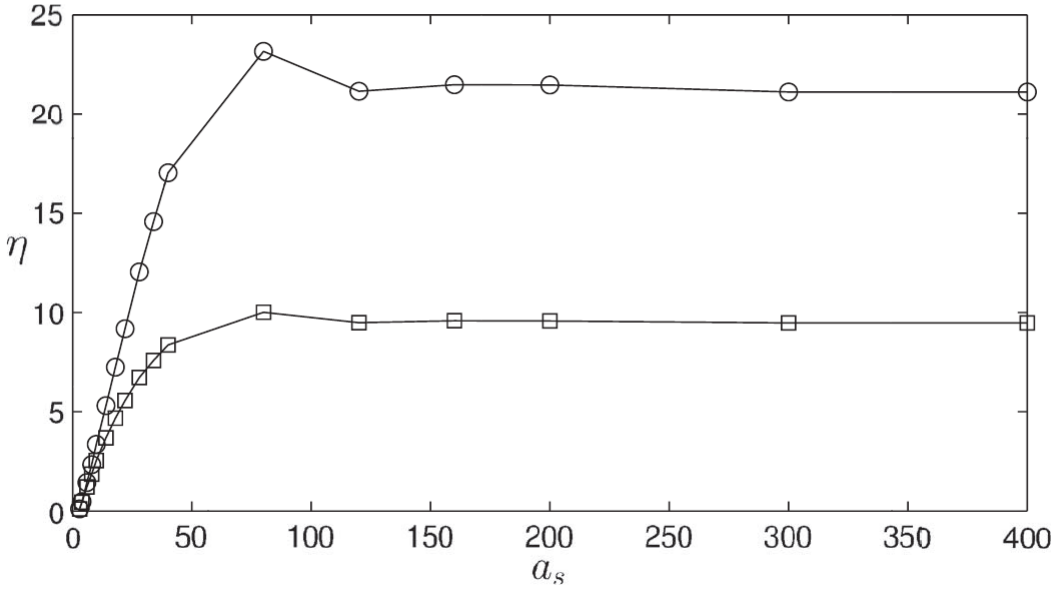

Figure 3.3: Graph of η against a_s. The circles represent data where η is a maximum, while squares where η is a minimum [15]

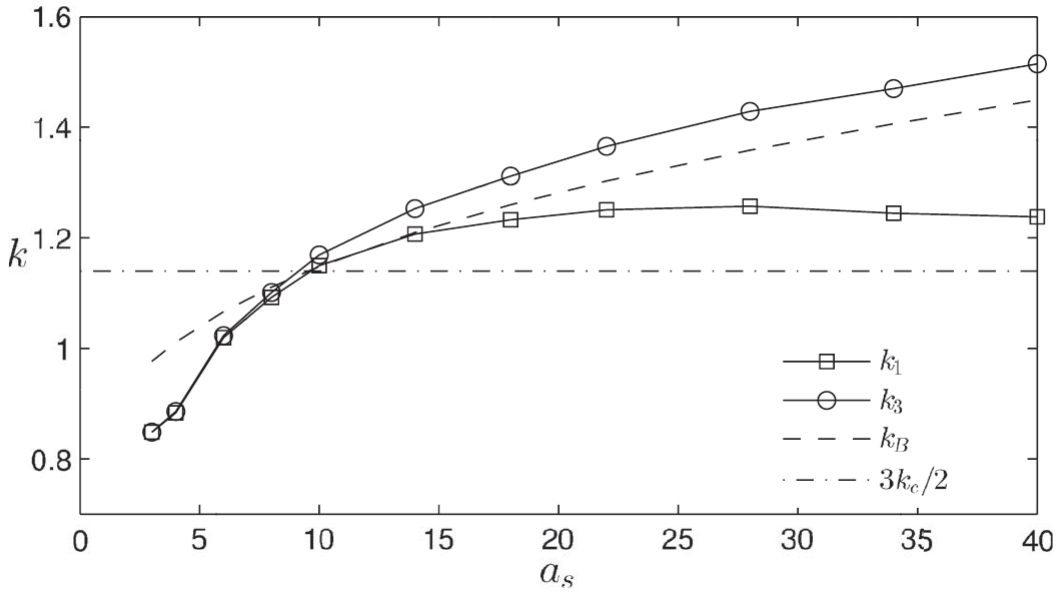

Figure 3.4: Graph of k against a_s. Squares and circles taken from numerical measurements [15]

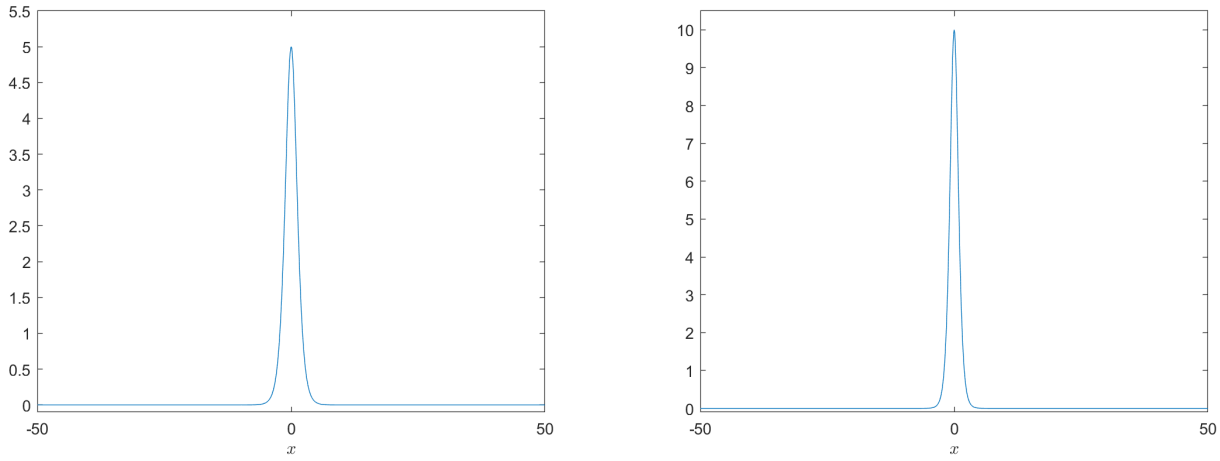

(a) (b)

Figure 3.5: Plot of the initial conditions used by Whitfield and Johnson with $a_s = 5$ (a) and $a_s = 10$ (b)

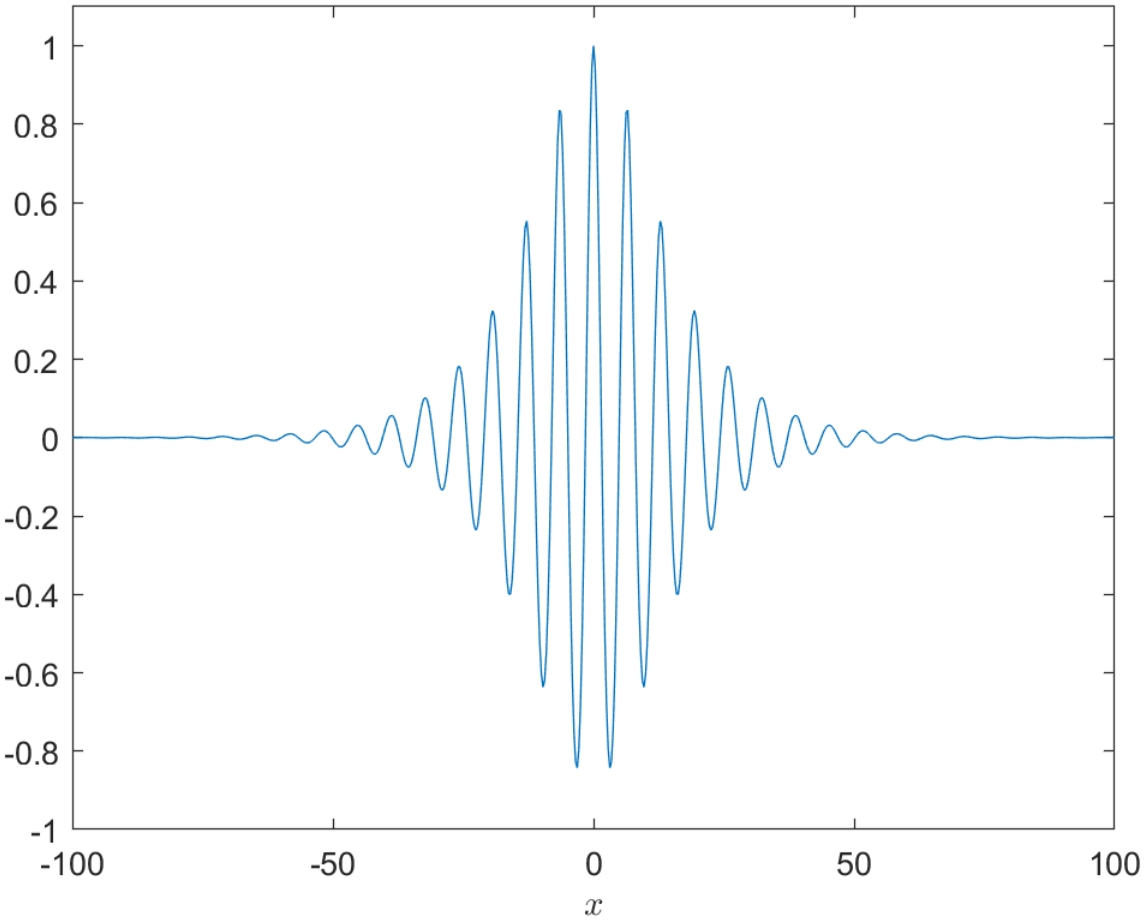

Figure 3.6: Plot of our initial conditions

3.7 Damping

During the integration, the equation generates some small-amplitude linear waves which radiate away from the solution. These appear because they are also solutions to the Ostrovsky equation, but since our solution is periodic in x, once the radiation reaches one of the boundaries, they re-appear from the other boundary and eventually, interfere with the wave-packet.

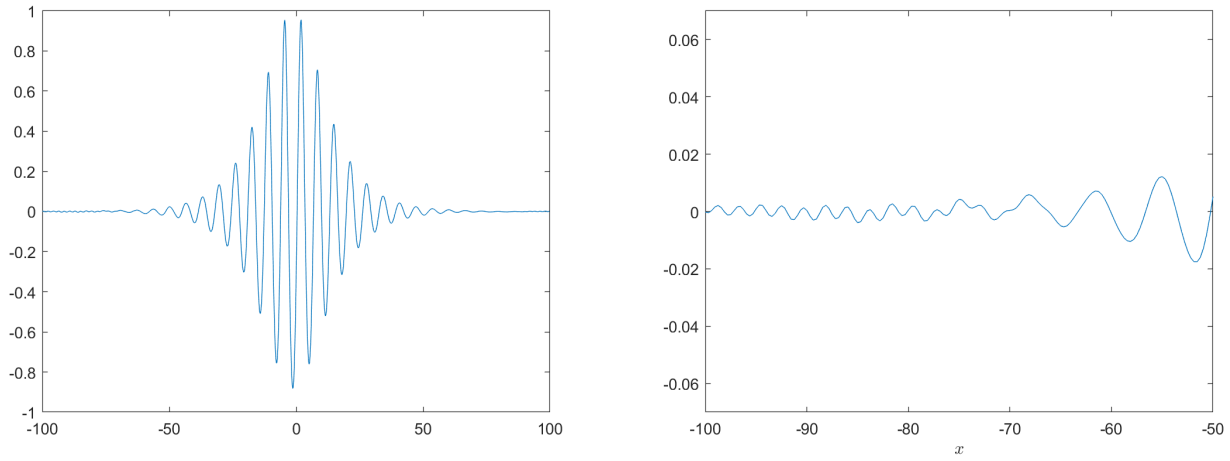

(a) (b)

Figure 3.7: Plot of the solution at $t = 4$ without damping

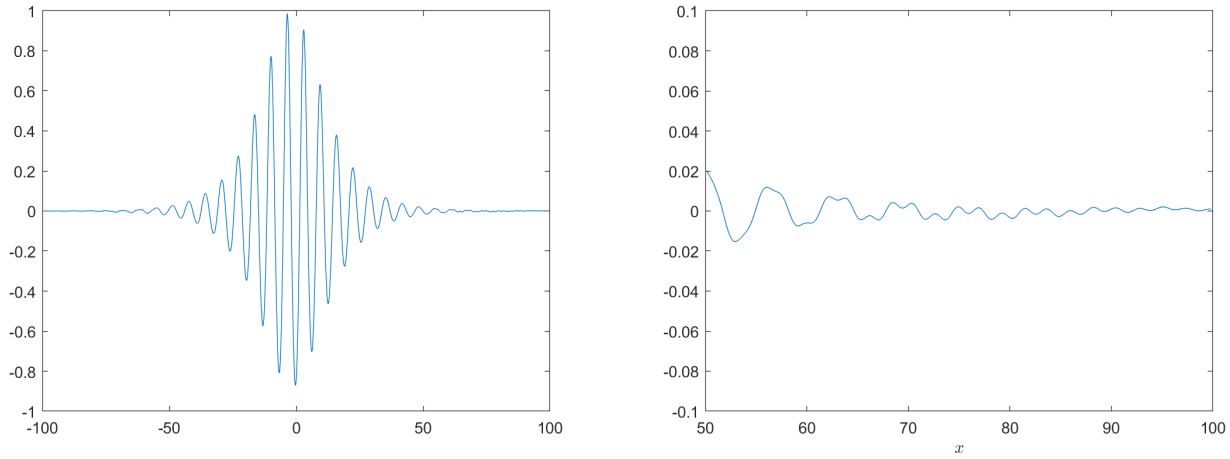

(a) (b)

Figure 3.8: Plot of the solution at $t = 6$ without damping

From Figure 3.7 and Figure 3.8, we can see exactly what we described above. We aim to find the period of the wave-packet and a good estimate for the value of the group velocity, but as the radiation reaches the wave-packet, its time-period changes. Therefore in order to perform more accurate measurements, we try to 'kill' this radiation by adding damping layers at the boundaries of our domain.

Consider the following PDE for the function $u(x, t)$

$$\frac{\partial u}{\partial t} = -mu \quad \text{where} \quad m > 0 \tag{3.7.1}$$

Which has the solution

$$u(x, t) = A(x)e^{-mt} \tag{3.7.2}$$

where A is a constant of integration in time.

We know that as t increases, the solution decays to zero as long as $A(x)$ has no singularities. Since our solutions do not contain such singularities, we can use this to make the radiation decay as they approach the boundaries by adding the term $-m\eta$ to the RHS of the Modified Ostrovsky equation. But the value m cannot be a constant, or else the solution would decay to zero uniformly across the x-domain, and the wave-packet would eventually disappear. Hence it must depend on x and it has to be positive across the x-domain in order to satisfy the decay condition. We therefore construct $m(x)$ in a way such that it forms a bump near the boundaries and it is almost zero everywhere else. If the x-domain has the form $[-L, L]$, we choose

$$m(x) = B\left[\exp\left(-\left(\frac{x-L}{C}\right)^2\right) + \exp\left(-\left(\frac{x+L}{C}\right)^2\right)\right] \tag{3.7.3}$$

where B and C are positive variables which we decide later in order to obtain a stable solution.

Figure 3.10 shows the results of the integration with the damping effect. At $t = 4$ (b) we can still see the radiation to the left of the wave-packet, while at $t = 10$ (d), the damping layer has partially dissipated the radiation. Finally when $t = 20$ (f), the radiation is completely gone and the wave-packet moves freely without any interference.

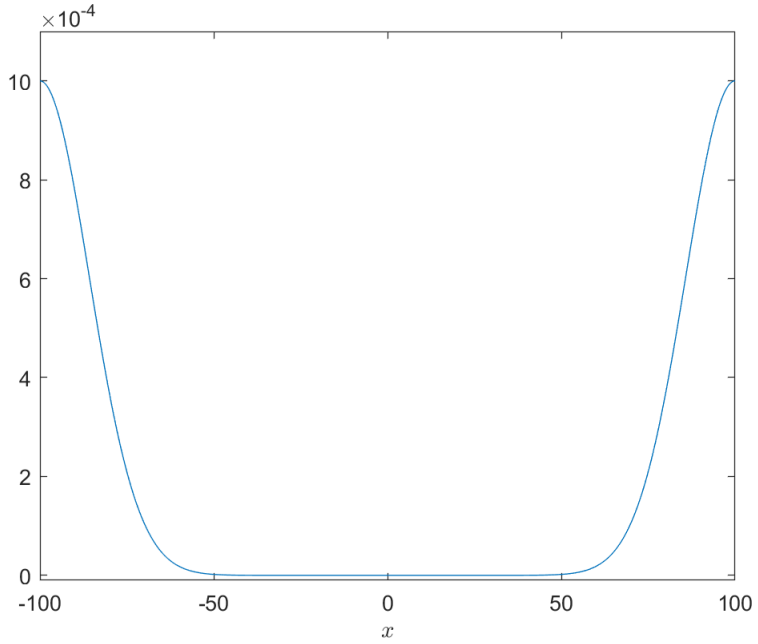

Figure 3.9: Plot of the damping function $m(x)$ for $L = 100$, $B = 0.001$ and $C = 20$

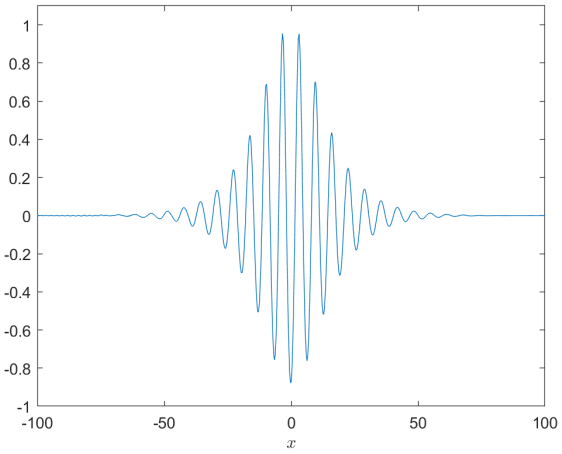

(a)

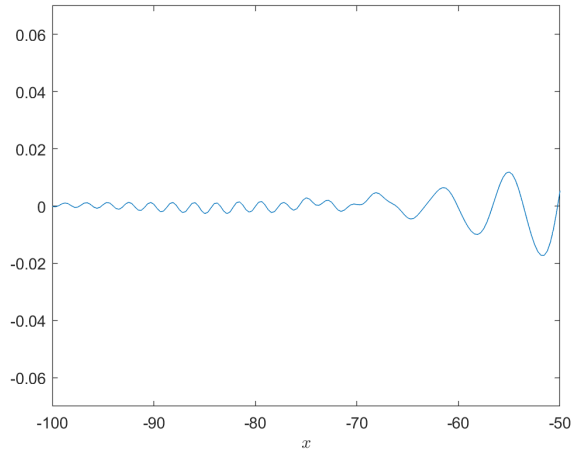

(b)

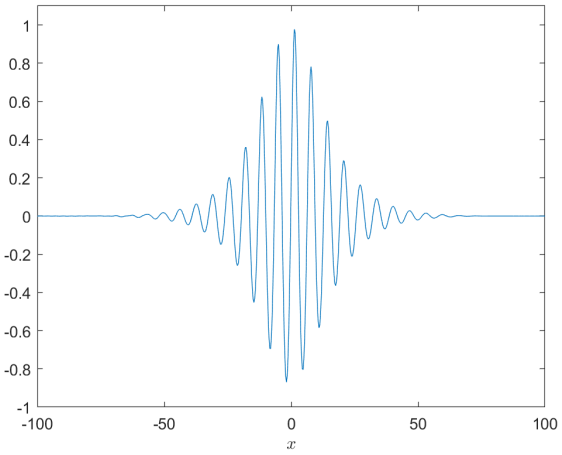

(c)

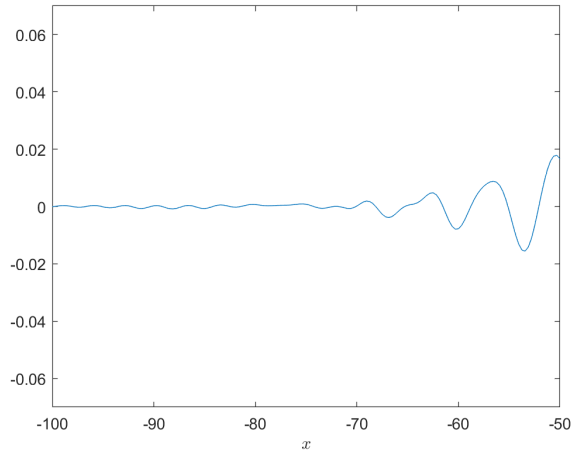

(d)

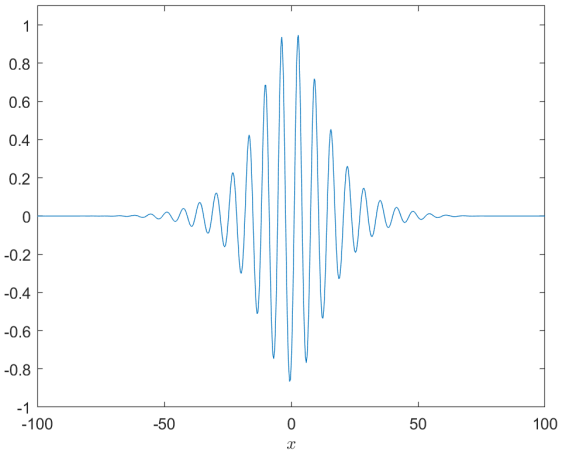

(e)

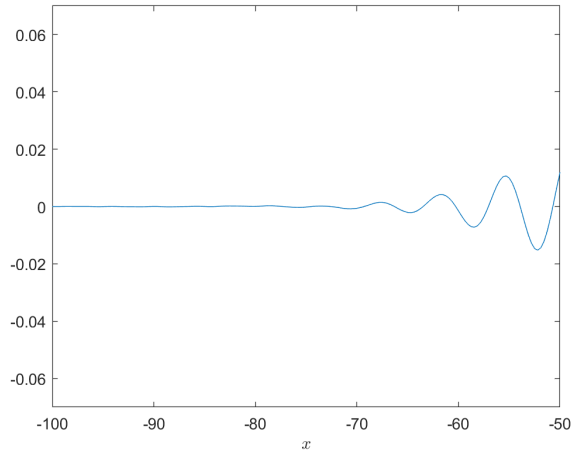

(f)

Figure 3.10: Plot of the solution with the damping effect at $t = 4$ (a), $t = 10$ (c) and $t = 20$ (e).

3.8 Measurements

In this section we will explain how we measured the time-period and the group velocity of the wave-packet solution.

The value of c_g found in Section 3.6 is simply an estimate of the true value of the group velocity, but we will use it to obtain a better approximation. At $t = 20$, our solution has no radiation and the program can start taking measurements. It first calculates the maximum value of the solution across the x-domain at each time-step, and then it finds at which position in x that value occurs.

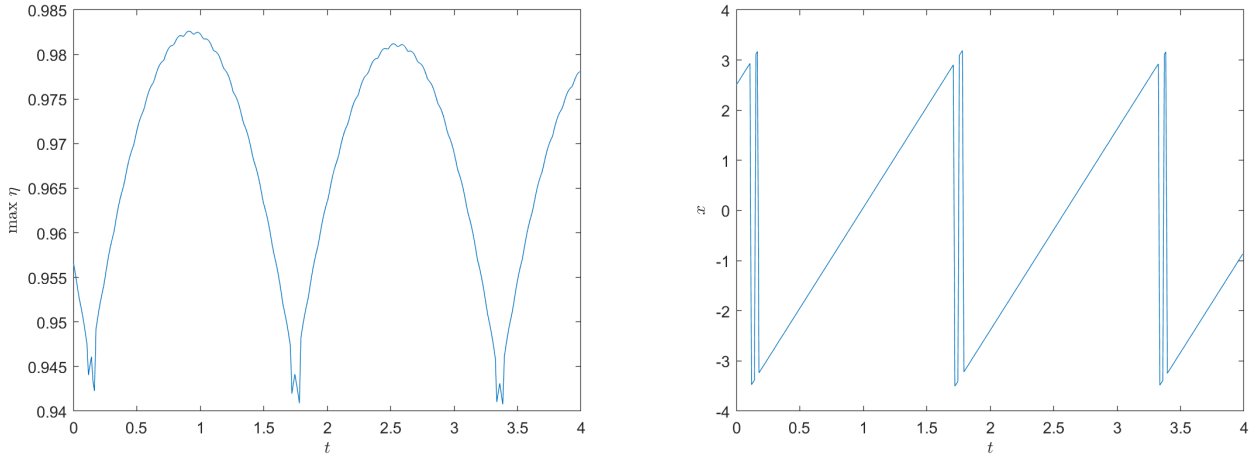

(a) (b)

Figure 3.11: Plots of the maximum value of the solution against time (a) and the position in x where that maximum occurs against time (b).

As we can see from Figure 3.11 (a), the plot of the maximum value of the solution over time forms peaks, and the difference in time when subsequent peaks reach their maximum should give the time-period of our solution. But this data is discretised, and therefore we will use interpolation to find a better estimate for the maximum values of these peaks. For each peak we are interested in three points: the point where the maximum value of the discretised data occurs, a point to its left and a point to its right. The interpolation consists in fitting a parabola between these three points, which is possible unless they are aligned. Now suppose these are given by (t_0, y_0), (t_1, y_1) and (t_2, y_2), where $t_0 > t_1 > t_2$. If they lie on the same parabola, then they satisfy the following system of equations:

$$\begin{aligned} a\ t_0^2 + b\ t_0 + c &= y_0 \\ a\ t_1^2 + b\ t_1 + c &= y_1 \\ a\ t_2^2 + b\ t_2 + c &= y_2 \end{aligned} \tag{3.8.1}$$

which in matrix form can be written as

$$\mathbf{T}_1 \mathbf{a} = \mathbf{y} \tag{3.8.2}$$

where

$$\mathbf{T}_1 = \begin{bmatrix} t_0^2 & t_0 & 1 \\ t_1^2 & t_1 & 1 \\ t_1^2 & t_1 & 1 \end{bmatrix}, \quad \mathbf{a} = \begin{bmatrix} a \\ b \\ c \end{bmatrix}, \quad \mathbf{y} = \begin{bmatrix} y_0 \\ y_1 \\ y_2 \end{bmatrix} \tag{3.8.3}$$

To find $\mathbf{a}$, we use Gaussian elimination which works unless the determinant of $\mathbf{T}_1$ is zero. This happens when

$$\begin{aligned} \det\mathbf{T}_1 &= t_0^2(t_1 - t - 2) - t_0(t_1^2 - t_2^2) + (t_1^2 t_2 - t_1 t_2^2) \\ &= (t_1 - t - 2)[t_0^2 - t_0(t_1 + t_2) + t_1 t_2] \\ &= (t_1 - t_2)(t_0 - t_1)(t_0 - t_2) = 0 \end{aligned} \tag{3.8.4}$$

i.e. when $t_0 = t_1$, $t_0 = t_2$ or $t_1 = t_2$. But by our assumption, $t_0 > t_1 > t_2$ and therefore Gaussian elimination never fails. In the case where the points lie on the same line, the program would simply return $a = 0$.

We may now find a better value for the time where the maximum value of the peak occurs by calculating $-b/2a$, for each of the two peaks and we denote them τ_1 and τ_2. Their difference will then give us an estimate for the time-period T:

$$\tau_2 - \tau_1 = T \tag{3.8.5}$$

Suppose now that the wave-packet moves with group velocity s. Within the frame where we introduce the moving coordinate $x \longrightarrow x - ct$, the packet then moves with speed $s - c$. Suppose further that the maximum of the two peaks arise at $x = m_1$ and $x = m_2$ so that when $t = \tau_1$ and $t = \tau_2$, the maximum of the solution is at $x = m_1$ and $x = m_2$ respectively. Then

$$s - c = \frac{m_2 - m_1}{T} \tag{3.8.6}$$

and after rearranging

$$s = c + \frac{m_2 - m_1}{T} \tag{3.8.7}$$

We therefore found a method to obtain better estimates for the value of the group velocity of the wave-packet.

We find m_1 and m_2 using Figure 3.11 (b). We know these values occur when $t = \tau_1$ and $t = \tau_2$, but as before, our data is discretised, so we will have to use interpolation again. We will show how we found m_1, but to find m_2 one can take the same steps. We know that τ_1 belongs to some interval $[t_n, t_{n+1}]$ in our time discretisation. If the maximum of the solution occurs at x_n and x_{n+1} when $t = t_n$ and $t = t_{n+1}$ respectively, then the point (m_1, τ_1) lies between (x_n, t_n) and (x_{n+1}, t_{n+1}), along the line joining these two points, and therefore satisfy the following system of equations

$$\begin{aligned} dt_n + e &= x_n \\ dt_{n+1} + e &= x_{n+1} \end{aligned} \tag{3.8.8}$$

which in matrix form becomes

$$\mathbf{T}_2\mathbf{d} = \mathbf{x} \tag{3.8.9}$$

where

$$\mathbf{T}_2 = \begin{bmatrix} t_n & 1 \\ t_{n+1} & 1 \end{bmatrix}, \quad \mathbf{d} = \begin{bmatrix} d \\ e \end{bmatrix}, \quad \mathbf{x} = \begin{bmatrix} x_n \\ x_{n+1} \end{bmatrix} \tag{3.8.10}$$

As before, we use Gaussian elimination to find $\mathbf{d}$, which works as long as the determinant of $\mathbf{T}_2$ is non-zero. But $\det\mathbf{T}_2 = 0$ when

$$t_n - t_{n+1} = 0 \tag{3.8.11}$$

and since $t_n \neq t_{n+1}$, Gaussian elimination functions perfectly.

The value for m_1 can be found via

$$m_1 = d\tau_1 + e \tag{3.8.12}$$

and m_2 is found similarly, as mentioned before.

We may may now find s by iterating (3.8.7) via the following iterations

$$s_n = s_{n-1} + \frac{m_{2_n} - m_{1_n}}{T_n} \quad \text{for} \quad n = 1, 2, 3, \ldots \tag{3.8.13}$$

where s_0 is given by our initial guess c_g found in Section 3.4.

The iterations proceed in the following way. At $n = 1$, we produce an initial guess for s_0, as described above. We integrate the Ostrovsky equation for some time after introducing the coordinates $x \longrightarrow x - s_0 t$. We then find values for T_1, m_{2_1} and m_{1_1} as explained earlier and consequently find s_1. We now integrate further the solution obtained after the first integration by the same amount of time as before, after introducing the new coordinate $x \longrightarrow x - s_1 t$. At this point, the program just repeats the process.

Figure 3.12 shows the results of our iterations. As we can see, iterations initially produce answers that spike up and down, but eventually these effects settle down and the iterations converge, slowly oscillating around a fixed value.

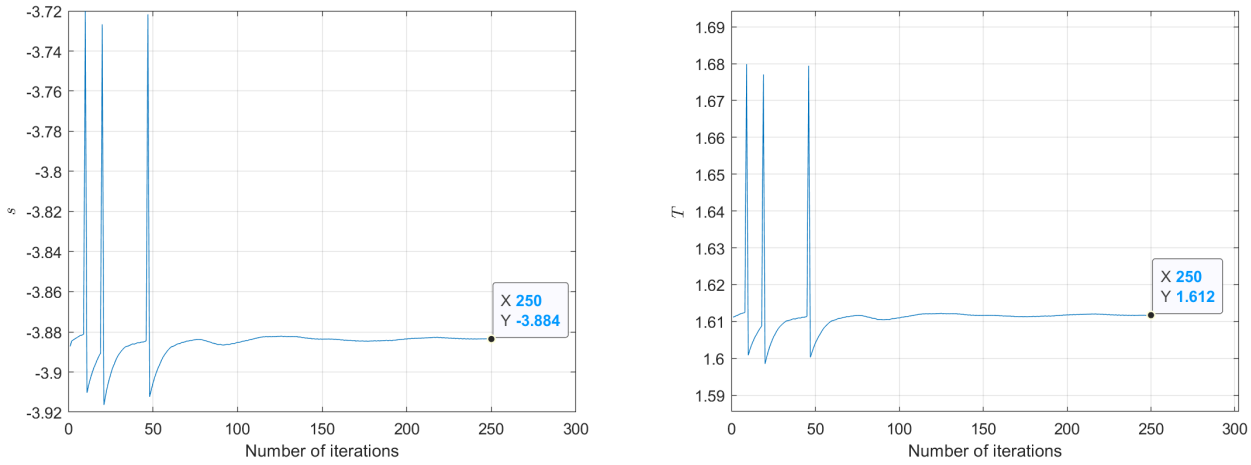

(a) (b)

Figure 3.12: Iterations results for the group velocity s (a) and for the time-period T (b).

Iterations give $T \approx 1.6117$ and $s \approx -3.8835$, which is not too far off from our initial guess $s_0 = c_g \approx -3.8872$. Hence c_g is a good estimate for the group velocity of this particular wave-packet.

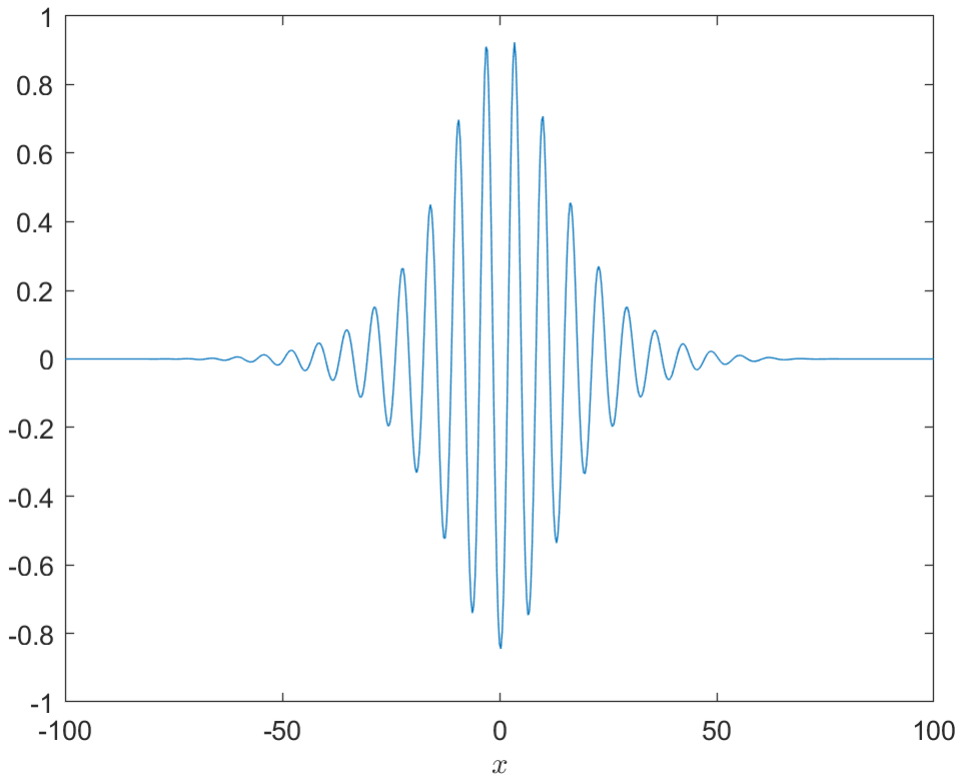

Figure 3.13: Solution after the iterations

Figure 3.13 shows the solution after the completion of the iterations. Its maximum amplitude has decreased a little, but we believe that it is due to the numerical integration. Other than that, the wave-packet travels with no problems.

3.9 Stretching the solution

We would like see if there exist non-linear wave-packet solutions of larger amplitude. In order to do this, we take the iterated solution found in the previous section and stretch it vertically across the domain. We do it by simply multiplying that solution by some positive value

$$\eta_{\text{new}} = p\ \eta_{\text{old}}, \quad p > 0 \tag{3.9.1}$$

where η_{new} will be the stretched solution, and η_{old} is the solution obtained at the end of the iterations in the previous section.

For our first attempt we used $p = 2$.

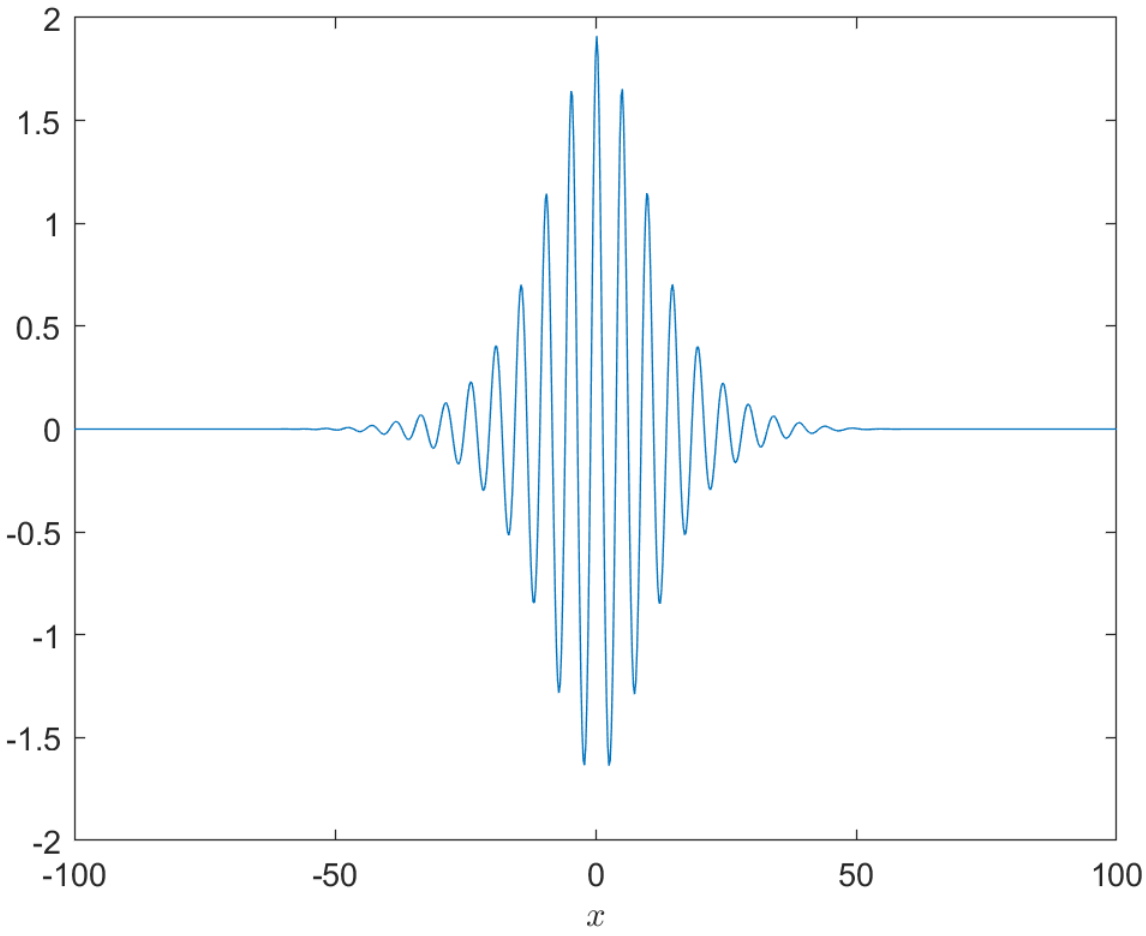

Figure 3.14: Stretched solution, $p = 2$.

We then performed the same measurements as in the previous section using the same iterations, but with a slight change in the damping function so that the solution would remain stable throughout the integration. we do this by either increasing or decreasing the values of B and C.

Figure 3.15 contains the results of these measurements. Again, the iterations converged after seeing the same spiky behaviour we saw earlier, yielding $s \approx -5.602$ and $T \approx 1.065$. Since we have found a solution with maximum amplitude larger than one, we believe that solutions with even larger amplitude can exist, and we can seek them by following the same approach we just did.

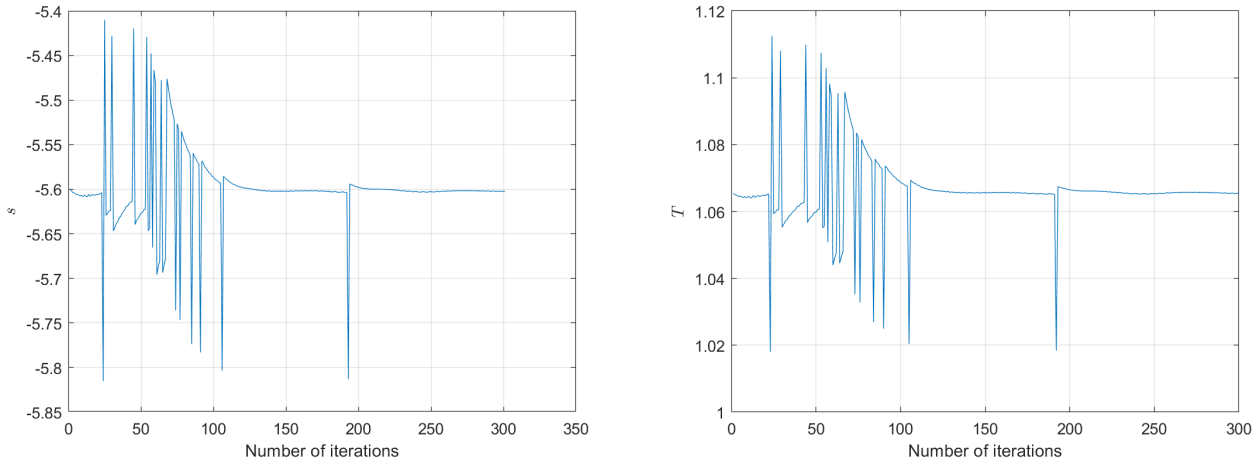

(a) (b)

Figure 3.15: Iterations results of the stretched solution for the group velocity s (a) and for the time-period T (b), $p = 2$.

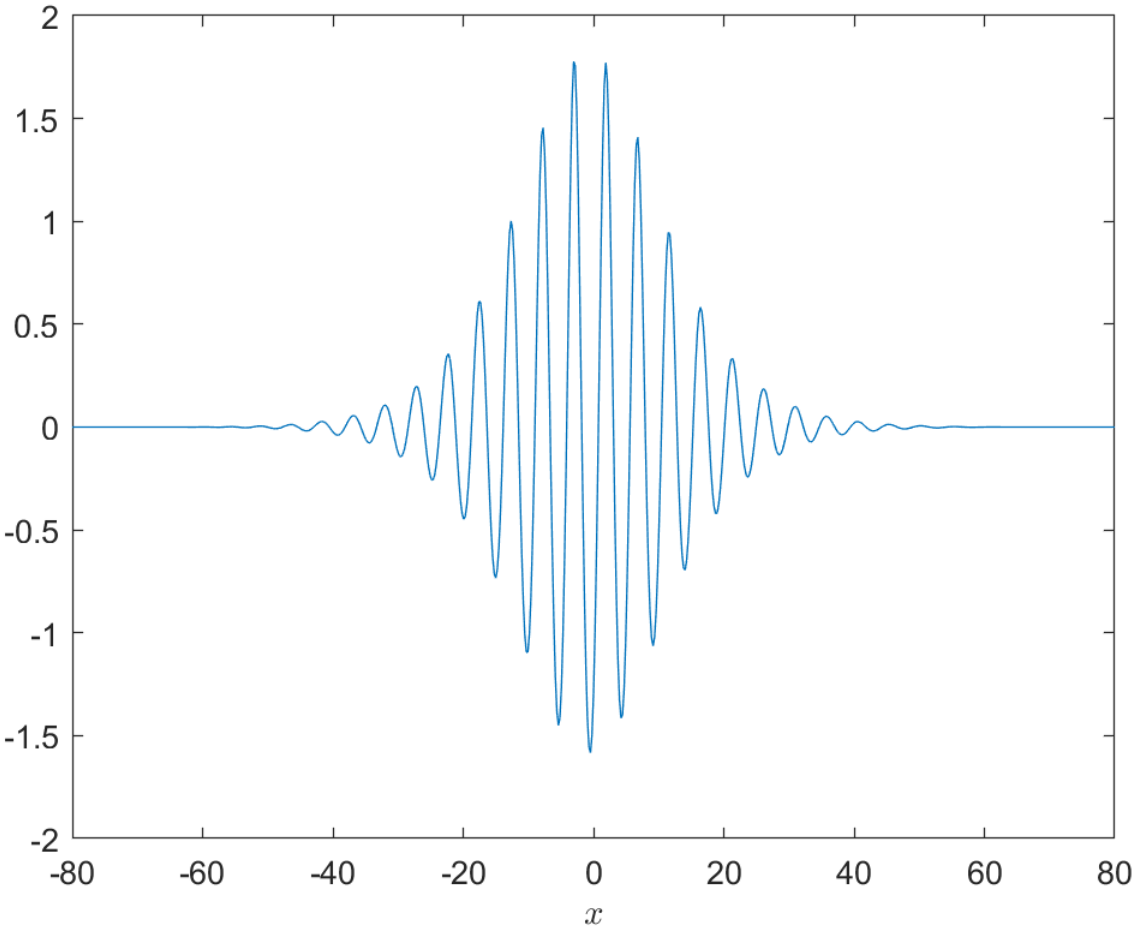

Figure 3.16: Stretched solution after the iterations, $p = 2$.

We then proceeded to stretch the wave-packet even further, using the solution shown in Figure 3.15 as η_{old} and $p = 2$ as before. Figure 3.16 shows the results of our measurements.

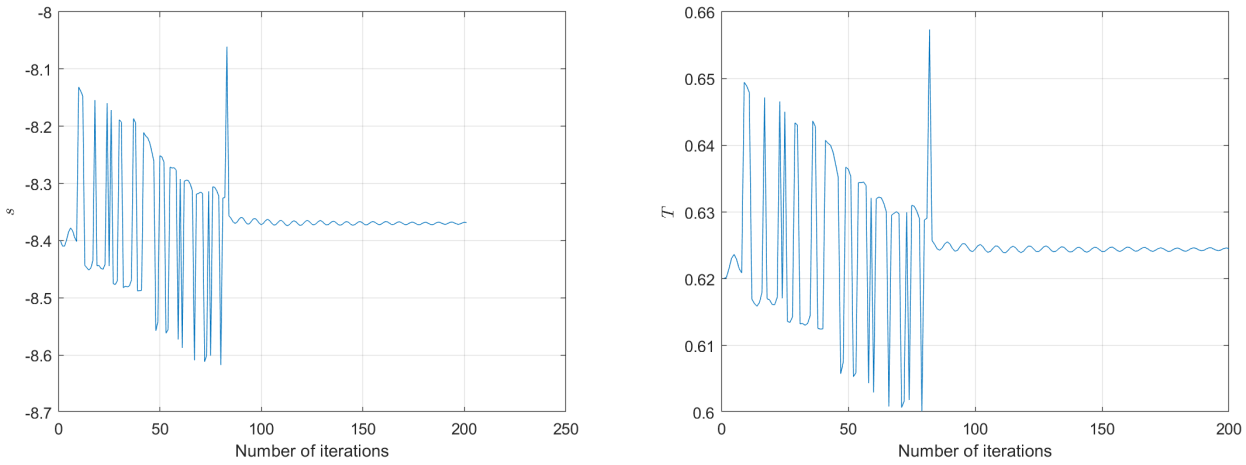

(a) (b)

Figure 3.17: Iterations results of the further stretched solution for the group velocity s (a) and for the time-period T (b), $p = 2$.

The values converge again, but unlike our previous attempts, the oscillatory behaviour in the convergence is more prominent this time, yielding

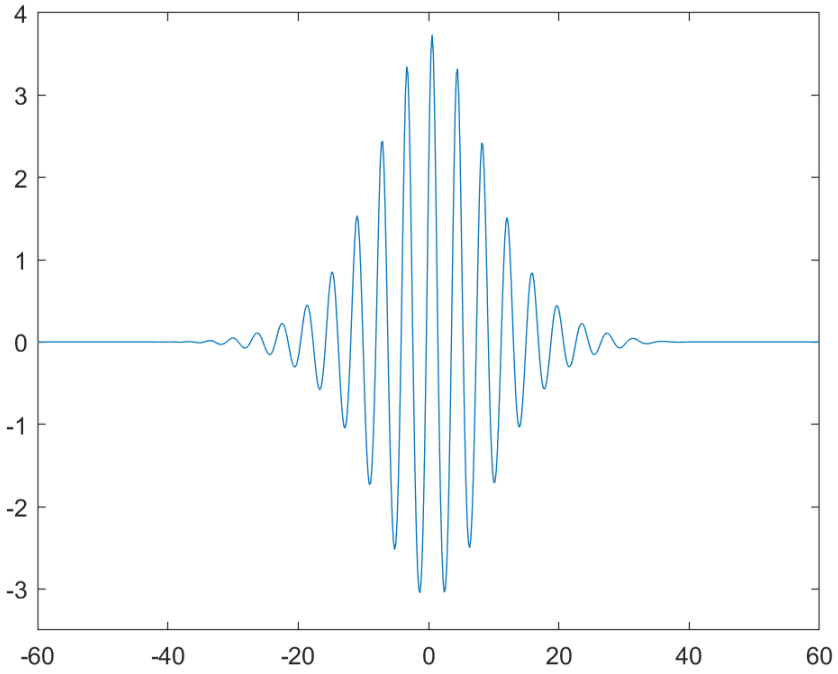

Figure 3.18: Further stretched solution after the iterations, $p = 2$.

This method seems quite strong. It allows us to find more solutions by increasing their size, but unfortunately, it is very impractical. For example, we realised that in order to obtain stable solutions where the maximum value of the amplitude doesn't decay as much as the ones we found, we needed to squash the wave-packet horizontally. Because of this, we also needed to readjust the damping function by strengthening (or weakening) and relocating it. Most of this was done via a trial and error which was very time consuming, and therefore this method is not very reliable.

Chapter 4

Future Work

As mentioned at the end of the last lecture, the method we came up with was not really reliable as it takes a lot of time to find new solutions of larger amplitude. The results showed that as we stretched the wave-packet, the group velocity increased in magnitude, while the time-period decreased. In order to see if this is also true for larger amplitude solutions, we need a more powerful method, which we describe in this chapter.

4.1 The continuation method

T.-S. Lin has in 2008 presented a method to find more travelling wave-solutions in x-domains of the form $[-L, L]$ [10]. The method consists in seeking solutions in the original problem, and from there they enlarge the x-domain by increasing the value of L, to see how that solution evolves in the new domain. This is known as a continuation method. They use the method to find solutions to equations of the form

$$\eta_t = (F[\eta])_x \tag{4.1.1}$$

where F is some non-linear differential operator. Recall that by (3.37), we may write the Ostrovsky equation as

$$\begin{aligned} \eta_t &= -\eta\eta_x - \eta_{xxx} + g(x,t) \\ &= (-\frac{1}{2}\eta^2 - \eta_{xx} + G(x,t))_x \\ &= (F[\eta])_x \end{aligned} \tag{4.1.2}$$

where G is an anti-derivative of g with respect to x.

Hence we have shown that the Ostrovsky equation is an equation of the form (4.0.1), and one can therefore use the continuation method to find its solutions in different x-domains.

In their method, s denotes the group velocity of the wave-packet, which they use by introducing the coordinate $x \mapsto x - st$. Equation (4.0.2) then becomes

$$\begin{aligned} \eta_t &= s\eta_x + (-\frac{1}{2}\eta^2 - \eta_{xx} + G(x,t))_x \\ &= s\eta_x + (F[\eta])_x \end{aligned} \tag{4.1.3}$$

They subsequently impose the following conditions

$$\int_{-L}^{L} \eta \sin(nqx)\ \mathrm{d}x = 0, \qquad q = \frac{\pi}{L} \tag{4.1.4}$$

$$\frac{1}{2L}\int_{-L}^{L} \eta\ \mathrm{d}x = \alpha \tag{4.1.5}$$

where n and α are chosen integers, to break the translational and volume symmetry respectively. With these conditions, one can then proceed to find the value of s, by first multiplying (4.0.3) by $\sin(nqx)$, and then integrate the equation from $-L$ to L. Now, since

$$\int_{-L}^{L} \eta_t \sin(nqx)\mathrm{d}x = \frac{\partial}{\partial t}\left(\int_{-L}^{L} \eta \sin(nqx)\mathrm{d}x\right) = 0 \tag{4.1.6}$$

we then obtain that

$$s = -\frac{\int_{-L}^{L}(F[\eta])_x \sin(nqx)\mathrm{d}x}{\int_{-L}^{L}\eta_x \sin(nqx)\mathrm{d}x} \tag{4.1.7}$$

They then seek a finite Fourier expansion type of solution of the form

$$\eta(x,t) = c_0(t) + \sum_{k=1}^{N}[c_{2k-1}(t)\cos(kqx) + c_{2k}(t)\sin(kqx)], \quad N > n \tag{4.1.8}$$

and conditions (4.0.3) and (4.0.4) lead to $c_0 = \alpha$ and $c_{2n} = 0$.

By applying the Fourier Transform to η, one can recover its Fourier coefficients, so applying the Fourier Transform to (4.0.3) gives the following system of ODEs

$$\dot{c}_i = \mathcal{N}_i(c_0, \ldots, c_{2n-1}, c_{2n+1}, \ldots, c_{2N}) \tag{4.1.9}$$

and one can integrate the above in time to obtain the Fourier coefficients of η at later times, where the initial conditions for (4.1.9) are obtained by applying the Fourier Transform to the initial guess for η. From there, one performs the Inverse Fourier Transform to these coefficients, to recover $\eta(x,t)$ for $t > 0$. The continuation then allows to find solutions for different x-domains.

They perform the continuation on Fortran by utilising the software AUTO07p with the FFTW3 package, but one can use the freely-available Matlab software package pde2path.

Unfortunately we did not have enough time to try out this method, but we believe that performing continuation using the wave-packets we found in Section 3.8 and 3.9, instead of the initial guess we used in Section 3.6, should give more accurate solutions in a less time-consuming manner. Because of this, we think that this method would allow a good extension to our project.

Appendix

Any codes used are available on my Github page: https://github.com/Calvin234/Wave-packets

Bibliography

[1] Internal waves in Quran. https://www.miracles-of-quran.com/internal_waves.html.

[2] Internal Waves Research. http://web.mit.edu/endlab/research/waves.html.

[3] Map of the South China Sea, political map. https://www.nationsonline.org/oneworld/map/South-China-Sea-political-map.htm.

[4] Alford M., Peacock T., MacKinnon J. et al. The formation and fate of internal waves in the south china sea. *Nature*, 521:65–69, 2015.

[5] David Farmer, Qiang Li, and Jae-Hun Park. Internal wave observations in the south china sea: The role of rotation and non-linearity. *Atmosphere-Ocean*, 47(4):267–280, 2009.

[6] R. H. J. Grimshaw, K. R. Helfrich, and E. R. Johnson. Experimental study of the effect of rotation on nonlinear internal waves. *Physics of Fluids*, 25(5):056602, 2013.

[7] Roger Grimshaw and Karl Helfrich. Long-time solutions of the ostrovsky equation. *Studies in Applied Mathematics*, 121, 07 2008.

[8] R. S. Johnson. *A Modern Introduction to the Mathematical Theory of Water Waves*. Cambridge Texts in Applied Mathematics. Cambridge University Press, 1997.

[9] Qiang Li and David M. Farmer. The generation and evolution of nonlinear internal waves in the deep basin of the south china sea. *Journal of Physical Oceanography*, 41(7):1345 – 1363, 01 Jul. 2011.

[10] T.-S. Lin, D. Tseluiko, M.G. Blyth, and S. Kalliadasis. Continuation methods for time-periodic travelling-wave solutions to evolution equations. *Applied Mathematics Letters*, 86:291–297, 2018.

[11] The Editors of Encyclopaedia. Internal waves. *Encyclopedia Britannica*, 2016.

[12] L. Pomar, M. Morsilli, P. Hallock, and B. Bádenas. Internal waves, an under-explored source of turbulence events in the sedimentary record. *Earth-Science Reviews*, 111(1):56–81, 2012.

[13] Y.A. Stepanyants. Nonlinear waves in a rotating ocean (the ostrovsky equation and its generalizations and applications). *Izv. Atmos. Ocean. Phys.*, 56:16–32, 2020.

[14] Lloyd Trefethen. Spectral methods in matlab. *SIAM*, 10, 01 2000.

[15] A. J. Whitfield and E. R. Johnson. Rotation-induced nonlinear wavepackets in internal waves. *Physics of Fluids*, 26(5):056606, 2014.